Elshazli *et al. J Infrastruct Preserv Resil* (2024) 5:5
https://doi.org/10.1186/s43065-024-00096-x

Journal of Infrastructure Preservation and Resilience

RESEARCH

Open Access

Advancing infrastructure resilience: machine learning-based prediction of bridges' rating factors under autonomous truck platoons

Mohamed T. Elshazli[3], Dina Hussein[2], Ganapati Bhat[2], Ahmed Abdel-Rahim[1] and Ahmed Ibrahim[1*]

Abstract

The operational characteristics of freight shipment will significantly change after the implementation of Autonomous and Connected Trucks (ACT). This change will have a significant impact on freight mobility, transportation safety, and the sustainability of infrastructure. Truck platooning is an emerging truck configuration that is expected to become operational in the future due to the rapid advancements in connected vehicle technology and autonomous driving assistance. The platooning configuration enables trucks to be connected with themselves and the surrounding infrastructure. This arrangement has shown to be a promising solution to improve the vehicles' fuel efficiency, reduce carbon dioxide emission, reduce traffic congestion, and improve transportation service. However, platooning may accelerate the damage accumulation of pavement and bridge structures due to the formation of multiple load axles within each platoon since those structures were not designed for such loads. According to AASHTO, bridges are designed based on a notional live load model comprised of one or two trucks per lane in conjunction with or separate from an applied uniform load (AASHTO, LRFD 2022). This damage, if accumulated, its repair would require billions of dollars from the government and would impede the movement of both people and goods. The potential damage to infrastructure may arise due to various factors such as the number of trucks in a platoon, gap spacing between trucks, and the type of trucks. This research work includes a thorough parametric study with 295,200 computer simulations using SAP 2000. The goal was to evaluate the effect of different truck platooning configurations on the load rating of existing bridges. The obtained results served as the dataset for training various machine learning models, including Random Tree, Random Forest, Multi-Layer Perceptron (MLP), Support Vector Regression (SVR), K-Nearest Neighbor (KNN), and Extreme Gradient Boosting (XGBoost). Results showed that Random Forest model performed the best, with the lowest prediction errors. The proposed machine learning model has shown its effectiveness in identifying optimal platooning configurations for bridge structures within the scope of the study.

Keywords Bridge, Platoon, Autonomous, Machine learning, Random forest, Load rating

*Correspondence:
Ahmed Ibrahim
aibrahim@uidaho.edu
Full list of author information is available at the end of the article

Graphical Abstract

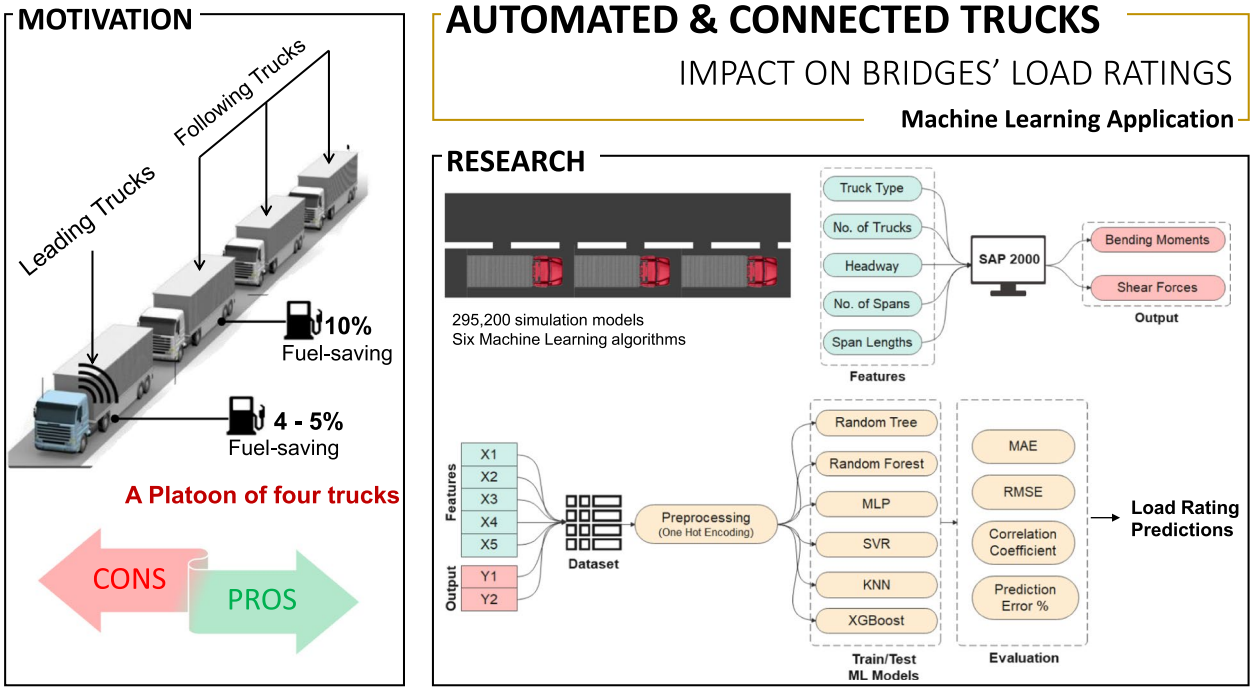

Introduction

The transportation sector has become the second-largest energy consumption section in the United States, with an oil demand of 52 million barrels per day [1]. Within the transportation industry, freight shipment represents a critical component that contributes significantly to overall energy consumption. Based on the International Energy Agency database (IEA, 2022), freight vehicles alone consumed 17 million barrels of oil per day, and this demand is expected to increase by 2.5 times by 2050 [2]. To address this growing concern, several innovative solutions have been proposed, including the use of wide-base tires [3], aerodynamic truck designs [4], and optimization of truck routes [5].

One potential solution that has gained significant attention is the platooning of freight trucks using autonomous and connected vehicle technology, where freight trucks are positioned close to each other to improve transportation efficiency. As illustrated in Fig. 1, a platoon is formed when trucks are placed very closely one after another, with a distance as close as 10 feet [6]. Platooning configurations utilize sensors to gather data that controls a

Fig. 1 A three-truck platoon (U.S. Department of Transportation)

truck's braking system and speed, ensuring safe and efficient operation. A forward collision avoidance system and vehicle-to-vehicle communication enable two trucks to travel closely together [7–9].

Truck platooning is expected to have numerous advantages in addition to reduced fuel consumption. This technology is expected to reduce traffic congestion, reduce carbon dioxide emissions, improve travel safety, and speed up goods delivery [8, 10–13]. By positioning trucks in platoon configurations with close inter-vehicle spacing, the total drag force experienced by each truck can be decreased [14, 15]. Consequently, this reduction in aerodynamic drag improves fuel efficiency and reduces fuel consumption, contributing to the environmental and economic benefits of truck platooning [16–18].

While truck platooning has the potential to improve transportation services and promote fuel efficiency, this innovative solution is expected to accelerate the deterioration of current infrastructure. The 615,000 bridges in the United States are designed to withstand the extreme forces produced by the hypothetical live-load model for the current conventional truck configuration. With the anticipated widespread adoption of Autonomous and Connected Trucks (ACT) technology, however, these bridges may become unsafe for operation [19, 20], necessitating the evaluation and load rating of all transportation infrastructure.

In 2017, the Florida Department of Transportation (FDOT) conducted a study that highlighted the need to improve load rating methodology to account for truck platooning with varying configurations and bridge conditions [21]. Kamaranian's 2018 study [22] evaluated the impact of different platoon configurations on the Hay River Bridge and reported that the bridge's load ratings were insufficient for three and four-truck platoons. Yarnold and Weidner's 2019 study [23] identified concerns for positive bending moments and shear forces in existing bridges designed according to AASHTO Standards Specification for Highway Bridges, which can limit the implementation of truck platooning. However, bridges designed according to AASHTO LRFD were found to be suitable for a wide range of platoon configurations. Tohme and Yarnold's 2020 study [24] on steel bridge load ratings using Florida C5 five-axle semi-tractor trailers found that bridges load rated using ASR and LFR experienced a reduction in their rating factors for bending moments and shear forces. On the other hand, bridges rated using LRFR did not show any issue with negative moment ratings, but they did experience a reduction in their rating factors for positive moments on longer spans with closely spaced trucks.

Thulaseedharan and Yarnold (2020) [25] developed a new methodology for prioritizing bridges for truck platooning implementation. This methodology was created to address the possible impact of truck platooning on bridges and to determine which bridges should be prioritized for renovation in order to accommodate this new technology. The Florida C5, Delaware T540, Alabama 3S2 AL, Kentucky Type 4, Mississippi HS-Short, and AASHTO Type 3S2 were among the six five-axle truck models studied. In 2021, Couto Braguim et al. [26] found that truck platooning led to high load effects, but it reduced fatigue damage due to the reduction in the number of stress cycles.

In our study in 2023 [20, 27, 28], a parametric study of 29,600 computer simulations was conducted. The study aimed to evaluate the influence of different truck platoon configurations, using the HS20 design truck, on the load rating of existing bridges using three different load rating approaches (ASR, LFR, LRFR). Bridges rated using ASR or LFR experienced a reduction in their rating factors for bending moments and shear forces. However, LRFR bridges showed better results, especially for short spans and widely spaced trucks. The findings showed significant variations in bridge rating factors, highlighting the need for further investigation of a wider range of platoon parameters.

The previously mentioned literature indicates the critical need for a simple and effective approach to identify appropriate platoon configurations for existing bridges. Structural analysis software usually demands substantial modeling efforts and computational resources. However, the evolution of machine learning (ML) techniques has allowed their application across a wide range of fields, as a tool for addressing challenging problems that are difficult to tackle using traditional approaches [29–33]. The use of ML techniques has a wide range of advantages, including their exceptional accuracy and robustness in formulating predictions for complex circumstances. Furthermore, while machine learning algorithms may require significant processing resources during the training phase, they ensure great computational efficiency during prediction, equivalent to empirical or semi-empirical formulas.

In this research work, we extended our earlier study by incorporating a wide range of truck platoon parameters, reaching a total of 295,200 computer simulations. The study matrix considered several parameters, including the number of bridge spans, span lengths, truck type, number of trucks, and spacing between trucks (headway). The results were analyzed to provide insight into the impact of various parameters on the rating factors of bridges. Furthermore, the obtained results served as the dataset for training various ML models, including Random Tree [34], Random Forest [35], Multi-Layer Perceptron (MLP) [36], Support Vector Regression (SVR) [37], K-Nearest Neighbor (KNN) [38], and Extreme Gradient

Boosting (XGBoost) [39]. ML models were used in conjunction with the AASHTO equations to predict the rating factors of bridges. "Numerical study results" section provides a comprehensive analysis of the parametric study to understand how the features correlate and how bridges' rating factors are affected by truck platooning. The performance of the different ML algorithms addressed in this study is discussed in "Machine Learning (ML) results" section. Finally, "Potential implementation" section provides case study bridges as practical examples of how the research approach can be applied.

Contributions: This paper makes the following contributions:

- Extending the previous research work by conducting a total of 295,200 computer simulations. This extension broadens the understanding of the truck platoon parameters influencing bridges' load rating.
- Providing a robust dataset for training ML models.
- Integrating ML algorithms with AASHTO equations to predict bridge rating factors. This integration represents a novel approach to improving the accuracy and efficiency of bridge rating assessments.

Research methodology

This study provides a tool that integrates ML models and AASHTO equations to predict percentage changes in bridge rating factors caused by truck platooning and provide optimal configurations. The methodology consists of two stages, Fig. 2. In the first stage, a numerical analysis was performed using SAP 2000 to compute the bending moments and shear forces of different parameters of the truck platoon, including the type of truck, the number of trucks, the headway spacing, the number of bridge spans, and the span length. The results served as a dataset for the second stage, which included the development and comparison of six ML regression models based on their accuracy. Finally, case study bridges were introduced to demonstrate the practical applicability of these models.

Numerical simulations

For this study, the same numerical model employed in our previous research work in [20, 27, 28] was utilized, with SAP 2000 v23.3.1 used for the analysis. The bridges were modeled as beam sections, with appropriate boundary conditions. Self-weights were ignored during the analysis. Moving loads were defined as 1144 load cases, each with varying types of trucks, number of trucks, and headway spacing. Moving-load analysis was used to compute influence lines, as well as envelope bending moment and shear force results, and all moving loads used a station step size of 1 ft to ensure accuracy. A MATLAB script was developed to generate the input data files and manage the multiple output outcomes. Three Comma-Separated Values (CSV) input files are required to define the model in SAP 2000: the bridge data file, vehicle definitions, and load cases. The MATLAB script was prepared to generate these files in a format compatible with SAP 2000 input CSV files. An overview of the methodology used in the MATLAB scripts to generate the files is provided in Table 1. The analysis method used in this study was validated by a study conducted by Sayed et al. (2020) [19]. Further details about the model and the validation results are shown in [20].

Parametric study

The study matrix considered several parameters, including the number of bridge spans, span lengths, truck type, number of trucks, and spacing between trucks (headway). By analyzing the results obtained from the simulations, we were able to evaluate the changes in bridge load ratings and make recommendations for future applications. Table 2 shows the parametric study matrix.

The selection of the number of spans for the present study was based on the National Bridge Inventory (NBI) database from 2022. The analysis revealed that bridges with more than four spans represented a small portion of the bridge population in the United States. The percentages of simple, two-, three-, four-, and more than four-span bridges in the Pacific Northwest states are shown in Fig. 3. The study, therefore, focused on four bridge cases, simple, two-, three-, and four-span bridges. The study of bridge continuity effects was considered through the analysis of the response of the two-, three-, and four-span bridges.

Several state departments of transportation (DOTs) have conducted extensive research to identify a truck that can effectively represent the various categories of trucks and reduce the uncertainty associated with live load calculations [40–42]. The Federal Highway Administration (FHWA) recently conducted a study that analyzed data from 49 Weigh-In-Motion (WIM) sites across 35 states to identify the most common truck configurations [43]. The results indicated that the five-axle tractor semitrailer Class 9 truck was the predominant class. Although Class 5 and Class 6 trucks were observed at some locations, accounting for up to 10.84 and 10.71 percent of total traffic, respectively, these trucks have fewer axles than Class 9 vehicles, resulting in reduced load effects. As a result, this study focused on analyzing various Class 9 truck configurations, including FHWA Class 9, NJTA Type 3S2, FDOT C5, AASHTO Type 3S2, ALDOT Type 3S2, Delaware T540, KYTC (Type 4), and MODOT (HS-Short) (see Fig. 4). Furthermore, the study considered platoons formed using the HS-20 design truck model, which is used in the ASD, LFD, and LRFD design methods.

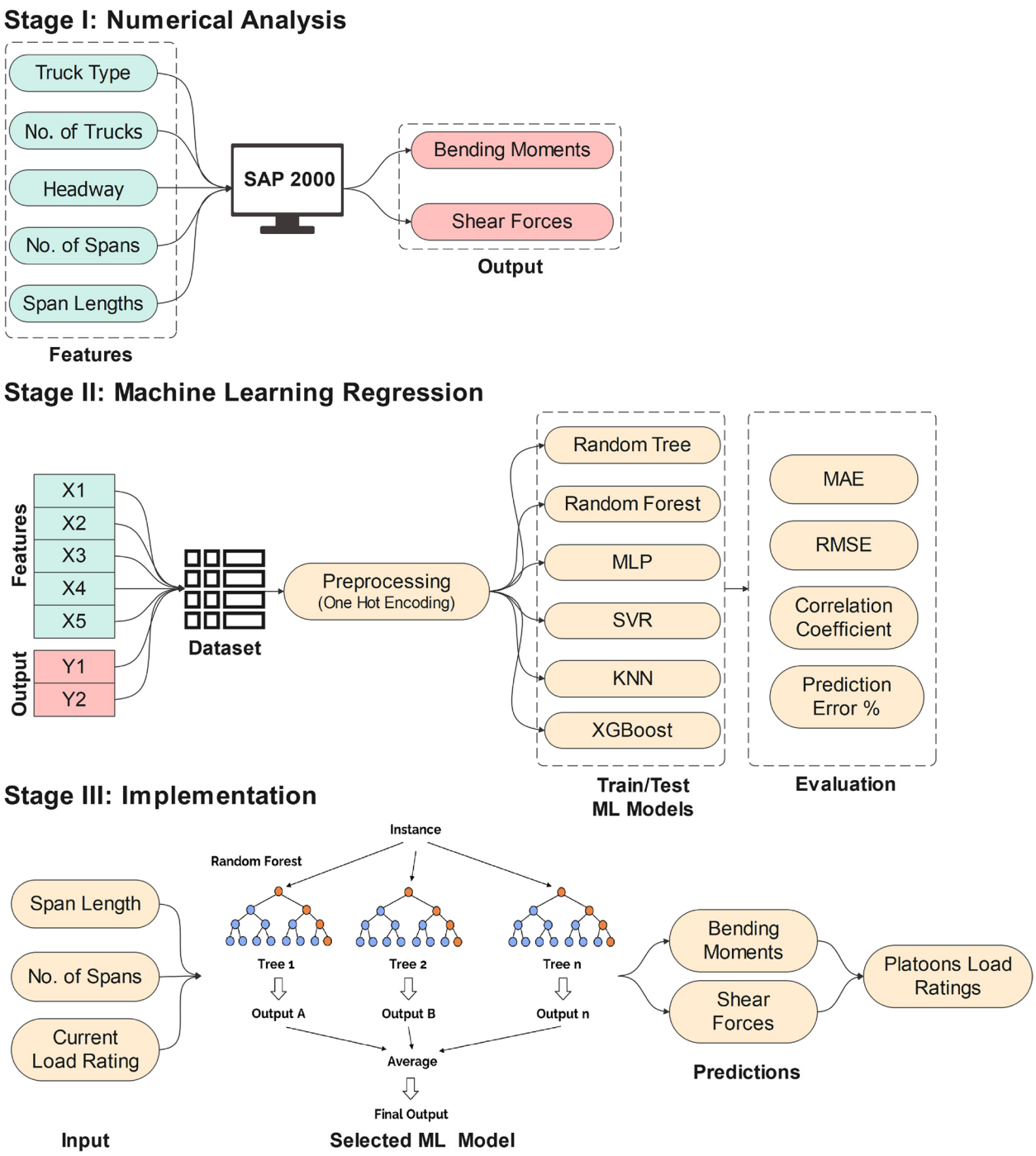

Fig. 2 Research methodology

The notional design live load HL-93 was used as the basis for evaluating the load ratings of bridges in this study. The HL-93 is made up of the HS20 design truck and a design lane load of 0.64 kip/ft, or tandem, in addition to the design lane load. It is important to point out that the HL-93 load model is adopted by the Load and Resistance Factor Design (LRFD) method. To ensure the safety and reliability of bridge structures under diverse loading conditions, the LRFD approach accounts for multiple load and resistance factors.

This study covers a wide range of truck platoons, up to 10 trucks, considering headway spacings between 8 and

Table 1 Data processing using MATLAB for SAP 2000 numerical analysis

Preprocessing:

Three Comma-Separated Values (CSV) input files were created using MATLAB to define the problem.

1) Bridge Data:

Variables: (number of spans (N), and span length (L))

1- Set the range of N and L according to the parametric study.

2- Loop over N and L to generate point coordinates, and frame elements.

3- Assign frame section.

2) Vehicle Definitions:

Variables: (number of trucks (x), number of axles (n), spacing between axles (s), and axle load (p))

1- Generate load names with the following designation (Type(class)_ Number(x)_Spacing(s)).

2- Assign number of axles for each load.

3- Define axle loads and spacing.

4- Apply scale factor (scale factor = 1 in the current study).

3) Load Cases:

1- Assign lanes to frame numbers.

2- Assign moving load cases for each load.

The three CSV dataframes are then imported into SAP2000

Postprocessing using MATLAB:

1- The results were exported in excel files.

2- MATLAB was used to perform the analysis and generate the figures.

Table 2 Parametric study matrix

Parameter	Number of variables	Increment	Range
No. of Spans	4	1	Simple Span - Four Spans
Span Length	41	5 ft	20 ft - 220 ft
Truck Type[a]	9	1	Type 1 - Type 9[a]
No. of Trucks	10	1	1 Truck - 10 Trucks
Headways	20	1 ft	10 ft - 30 ft

[a] Truck types details are shown in Fig. 4

30 ft. The headway spacing is the distance between the last axle of the leading truck and the first axle of the following truck. Previous research has determined that a minimum safe distance between trucks of 10 ft (approximately 3 meters) is necessary [27, 44]. However, with the growing improvement of this technology, headway spacing is expected to be as short as 8 ft. This range of headway spacing is essential to evaluate the effects of different distances between trucks in a platoon formation.

Bridge load ratings

The bridge load rating is an important method used by bridge owners to evaluate the current state of a bridge and its capacity to carry a live load. The rating factor (RF) is calculated by subtracting the dead load demand from the capacity and dividing the result by the live load demand.

The primary aim of this research was to develop ML models applicable to bridges designed according to ASD, LFD, and LRFD. It is recognized that bridge details, such as material and cross section, are required to calculate element capacity, and dead loads, to determine bridge rating factor according to LRFR, LFR, and ASR, using Eqs. 1 and 2.

$$\mathrm{RF_{LRFR}} = \frac{\mathrm{C} - \gamma_{\mathrm{DC}}.\mathrm{DC} - \gamma_{\mathrm{DW}}.\mathrm{DW}}{\gamma_{\mathrm{LL}}.(\mathrm{LL} \times \mathrm{IM})} \tag{1}$$

where C is the capacity, DC is the dead load, DW is the wearing surface load, LL is the live load, IM is the dynamic effect, γ_{DC}, γ_{DW}, and γ_{LL} are load factors.

$$\mathrm{RF_{ASR-LFR}} = \frac{\mathrm{C} - \mathrm{A_1}.\mathrm{D}}{\mathrm{A_2}.\mathrm{L}(1 \times \mathrm{I})} \tag{2}$$

where I is the capacity, D is the dead load, L is the live load, I is the dynamic effect, $\mathrm{A_1}$, and $\mathrm{A_2}$ are load factors.

While computing the rating factors for existing bridges using design loads (HS20 and HL93) is relatively straightforward, calculating the impact of various truck platooning configurations on bridge rating factors is time-consuming and costly. This requires an extensive numerical study to identify the optimal configurations, adding a layer of complexity to the analysis. Therefore, our study did not focus on absolute rating factors, but on finding the percentage change in rating factors. In order to calculate the percentage change in rating factors, element capacity and dead loads will remain constant, and be eliminated from the equation. The final equations were just functions of the live loads, which were determined through the parametric study, see Eqs. 3 and 4.

$$\%\Delta\mathrm{RF_{LRFR}} = \left(1 - \frac{\mathrm{LL_{HL93}} \times \mathrm{IM}}{\mathrm{LL_{Platoon}} \times \mathrm{IM}}\right) \times 100 \tag{3}$$

where $\Delta\mathrm{RF_{LRFR}}$ is the percent of change in LRFR, $\mathrm{LL_{HL93}}$, and $\mathrm{LL_{Platoon}}$ are the live loads due to HL93 design live load and a platoon configuration, respectively, IM is the dynamic effect.

$$\%\Delta\mathrm{RF_{ASR-LFR}} = \left(1 - \frac{\mathrm{LL_{HS20}} \times (1 + \mathrm{I})}{\mathrm{LL_{Platoon}} \times (1 + \mathrm{I})}\right) \times 100 \tag{4}$$

where $\Delta\mathrm{RF_{ASR-LFR}}$ is the percent of change in ASR or LFR, $\mathrm{LL_{HS20}}$, and $\mathrm{LL_{Platoon}}$ are the live loads due to HS20 design live load and a platoon configuration, respectively, I is the dynamic effect.

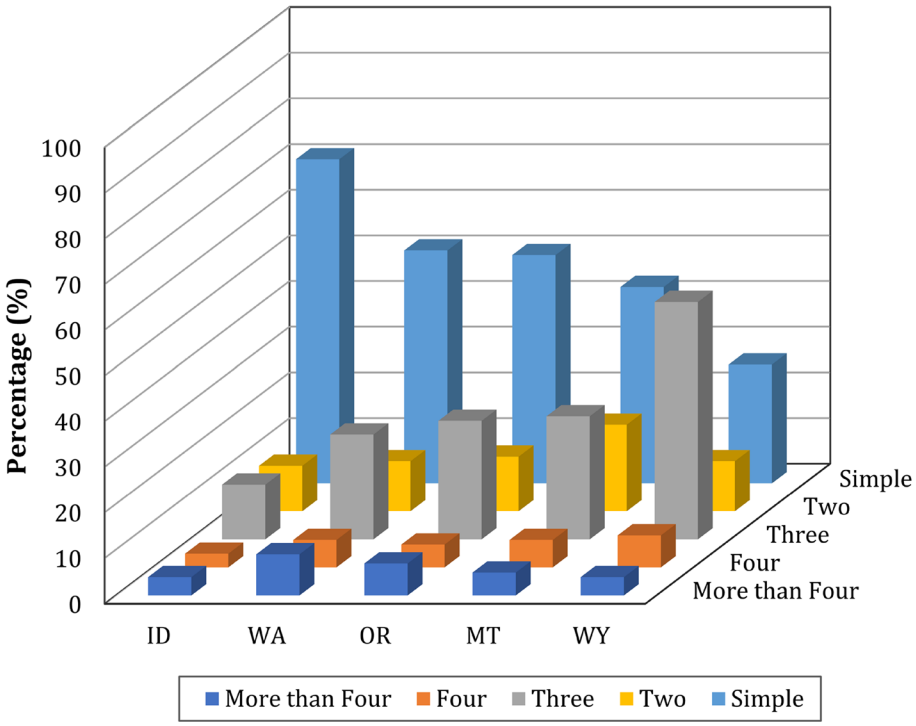

Fig. 3 Percentages of simple, two, three, four, and more than four-span bridges in the Pacific Northwest states

Numerical study limitations

The analysis is limited to superstructures designed using HS20 or HL93, and further research is needed to evaluate the substructure systems. In addition, the study assumes that all continuous-span bridges have equal spans. Another important assumption is that the platoon formation only involved trucks of the same type with constant headway spacing, without considering the impact of breaking force on the bridge. Lastly, the potential effects of combining truck platoons with regular traffic were not explored in this study. These limitations and assumptions must be kept in mind when applying the findings to real-world scenarios.

Dataset and feature selection

For the purpose of developing a robust ML model, a comprehensive dataset was utilized, which was obtained through the numerical simulation step. We fed five features to the ML model, x_1 to x_5, representing: truck type, number of trucks, spacing between trucks (headway), number of spans, and span length. While training, we also provided the model with output $y_i (i \in \{1, 2, 3\})$ which is either positive or negative bending moment or shear force. A separate model was trained for each output. The complete database is provided upon request.

Machine learning models

Six ML regression algorithms were adopted in this study to develop a predictive model: (1) Random Tree , (2) Random Forest, (3) Multi-Layer Perceptron (MLP), (4) Support Vector Regression (SVR), (5) K- Nearest Neighbor (KNN), and (6) Extreme Gradient Boosting (XGBoost). For the first three models, we used WEKA platform [45] for training and validation. For algorithms (4) and (5), we used scikit-learn library [46] in Python. For XGBoost algorithm, we used the XGBoost library [47] in Python.

One-hot encoding was used to represent the truck type in a binary vector. One-hot encoding is a popular ML technique used to represent categorical variables as binary vectors [48]. Each category is transformed into a binary vector with a one in the position corresponding to the category and zeros in all other places, allowing categorical data to be used effectively in ML algorithms.

To ensure the validity of the ML models, It is crucial to separate training and testing data. Two commonly used methodologies for training and test data separation include k-fold cross-validation and data splitting. k-fold cross-validation splits available data into k equal parts and trains the model k times. One data split among the k splits is used for testing while others are used for training. After verifying robustness of training and ensuring that all models provide comparable accuracy, the best

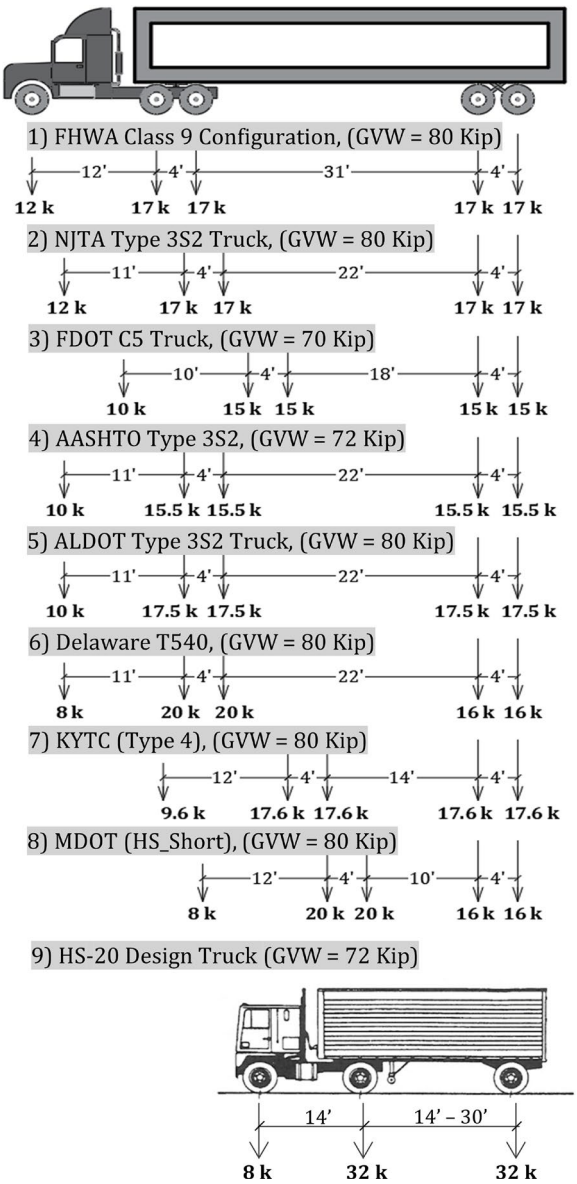

Fig. 4 Truck types included in the parametric study

performing model among the k trained models is used for testing with the entire dataset. The second approach for model training splits available data into dedicated training and test sets. The test set is hidden during model training and is used to evaluate performance of the trained model on unseen data. We used cross-validation in the Weka platform with 10 folds. In Python, the data was split into 60% for training and 40% of the dataset for testing. We evaluate the models with the entire dataset after training using several performance measures including Root Mean Square Error (RMSE), Mean

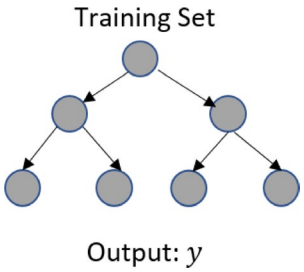

Fig. 5 Schematic Diagram of Random Tree Algorithm

Absolute Error (MAE), and Correlation Coefficient (r). The RMSE and MAE are defined as:

$$RMSE = \sqrt{\frac{1}{n}\sum_{i=1}^{n}(y_i - \hat{y}_i)^2} \tag{5}$$

$$MAE = \frac{1}{n}\sum_{i=1}^{n}|y_i - \hat{y}_i| \tag{6}$$

where n, y_i, and $\hat{y}_i$ represent the total number of data points, actual values of the target variable, and predicted values of the target variable. Similarly, the correlation coefficient is defined as:

$$r = \frac{\sum_{i=1}^{n}(x_i - \bar{x})(y_i - \bar{y})}{\sqrt{\sum_{i=1}^{n}(x_i - \bar{x})^2}\sqrt{\sum_{i=1}^{n}(y_i - \bar{y})^2}} \tag{7}$$

where x_i, $\bar{x}$, and $\bar{y}$ are values of the first variable, mean of the first variable, and mean of the second variable, respectively. The equation calculates the ratio of the covariance between the two variables and the product of their standard deviations, resulting in the correlation coefficient r.

Random tree

Random Tree is an ensemble learning tree-like model algorithm of decisions and their consequences. The architecture of the algorithm is composed of nodes and leaf nodes, where nodes represent decision points based on attribute values, and leaf nodes represent the final predicted outcome as seen in Fig. 5. It adopts the idea of random feature selection and bootstrap aggregating [34]. It is widely used for classification and regression tasks.

A random tree was trained with a total number of nodes of 12965 to predict the positive bending moment, negative bending moment, and shear force. One tree is trained to predict each metric. Each tree considers three randomly chosen features at each node. We used in our experiment on WEKA a batch size of 100. The minimum proportion of the variance on the data that needs to be

present at a node in order for splitting to be performed was set to 0.001.

One limitation of random trees is that they may suffer from overfitting a set of training data where the model has high accuracy on the training data but fails to generalize to new data. This is because the model memorized training data and failed to learn the underlying pattern that is applicable to new data [49]. Therefore, other algorithms such as random forest and XGBoost were explored to limit overfitting.

Random forest

Random forest algorithm has been used by researchers to avoid data overfitting [35]. Random forest combines multiple decision trees (bagging) to improve prediction accuracy and reduce overfitting. Each tree is built from a random subset of the training data and a random subset of the features. The final prediction is aggregated from individual tree results by utilizing the principle of majority voting for classification tasks and averaging for regression tasks, as shown in Fig. 6. In the experiment on WEKA, we used 100 trees with a total size of 10811 nodes. We utilized bagging with about 100 iterations.

Multi-Layer Perceptron (MLP)

MLP algorithm is a widely used artificial neural network architecture. It consists of multiple layers of interconnected artificial nodes which are called neurons, organized in a feedforward manner [36]. The term "feedforward neural network" refers to information flowing from the input layer to the output layer in the network structure without any feedback or loop connections. Each neuron takes weighted inputs, applies an activation function to the sum, and then propagates the output to the neurons in the following layer. Figure 7 illustrates the basic structure of a feed-forward multi-layer perceptron model. MLPs have shown good performance in learning non-linear relationships for classification or regression tasks [36]. In WEKA, the number of hidden layers is set as one.

The nodes in this network used Sigmoid activation function which takes an input value and transforms it into a number between 0 and 1. Since we formulated a regression problem with a numeric output, the activation function in the output was set to linear units in order to obtain continuous output values instead of bounded values to a specific range. Validation threshold technique was used for set-based early stopping. This means separate validation dataset is used to monitor the model's performance during training. The training process is stopped if the model's performance on the validation set starts to degrade, indicating overfitting. We used a validation threshold of 20 for this network and a momentum applied to the weight updates of 0.2. The number of epochs to train was 500 with a learning rate of 0.3 and a batch size of 100.

Support Vector Regression (SVR)

SVR is a variant of the well-known support vector machine algorithm [37]. The hyperplane, that fits the training data, is determined via support vectors, which are subsets of the training data that exhibit the closest proximity to the hyperplane. The margin represents region where the model is confident about the predictions. The model produced by SVR targets a hyperplane that does not exceed ϵ, as seen in Fig. 8. There are a variety of formulation Kernels that a SVR can use, where the kernel determines shape of the decision boundary. We used Radial Basis Function (RBF) kernel from the scikit-learn library [46] for the SVR model. The RBF kernel is useful in fitting non-linear regression models by transforming the input features to a higher-dimensional space where nonlinear and complex relationships can be effectively captured. It can be expressed as: $K(x, x') = \exp\left(-\|x - x'\|^2\right)$ where $K(x, x')$ represents the RBF kernel between two input vectors x and x', exp denotes the exponential function, and $\|x - x'\|^2$ denotes the squared Euclidean distance between the input vectors.

K- Nearest Neighbor (KNN)

KNN is a non-parametric algorithm for predicting numerical values [38]. The concept is to estimate the value of a variable, by averaging the the values of its k nearest neighbors. The hyperparameter K is chosen carefully to balance the bias-variance trade-off. The nearest neighbor is determined by measuring the distance between the variable and the rest of the k points. The distance metric measures dissimilarity or similarity between two data points in the feature space to evaluate how close or far apart the points are. The choice of distance such as Euclidean or Manhattan distance is another factor that can affect the calculation of the data point. The choice depends on the characteristics of the data and the problem domain. For example, Euclidean distance is best used for continuous data where on the other hand, Manhattan distance is used for discrete data. In this experiment, we used the scikit-learn library [46] from Python with a k of five. We also chose Euclidean distance since the data are continuous in our case. Euclidean distance calculates the straight line distance between two points in a 2D Cartesian coordinate system as follows:

$$d = \sqrt{(x_2 - x_1)^2 + (y_2 - y_1)^2}$$

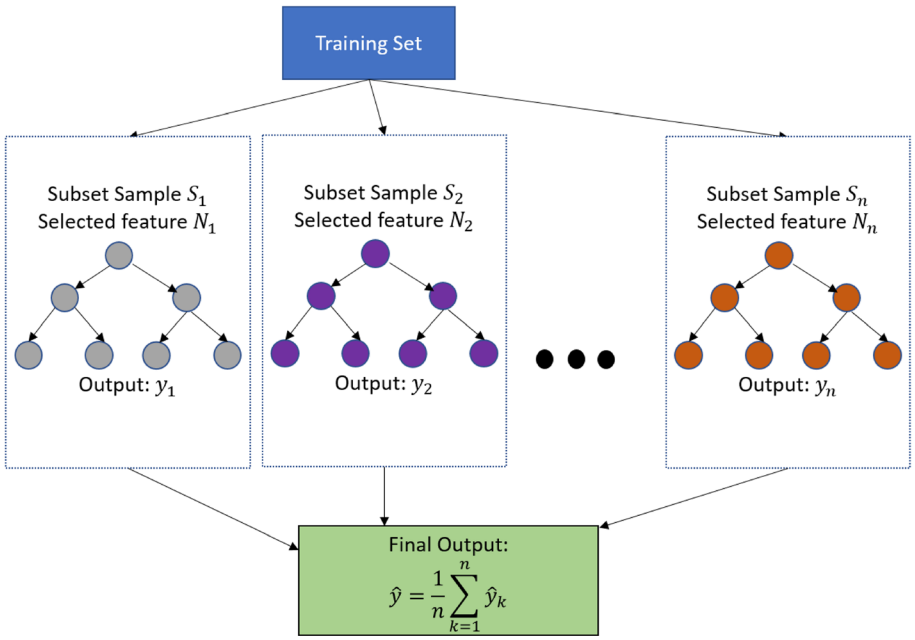

Fig. 6 Schematic diagram of random forest algorithm

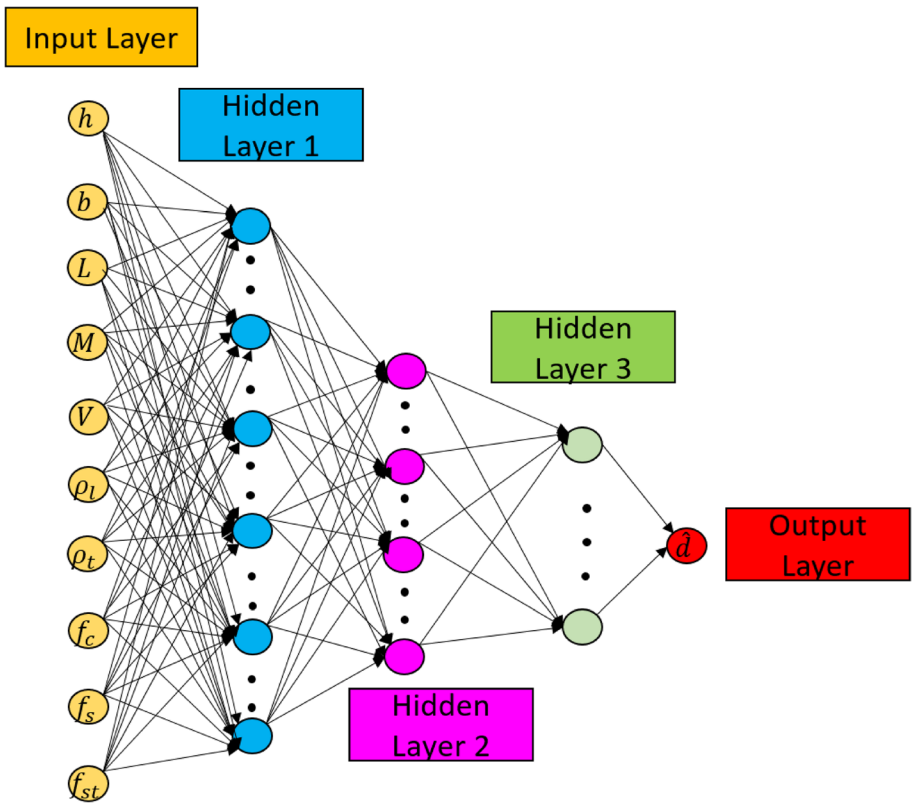

Fig. 7 Schematic diagram of MLP algorithm

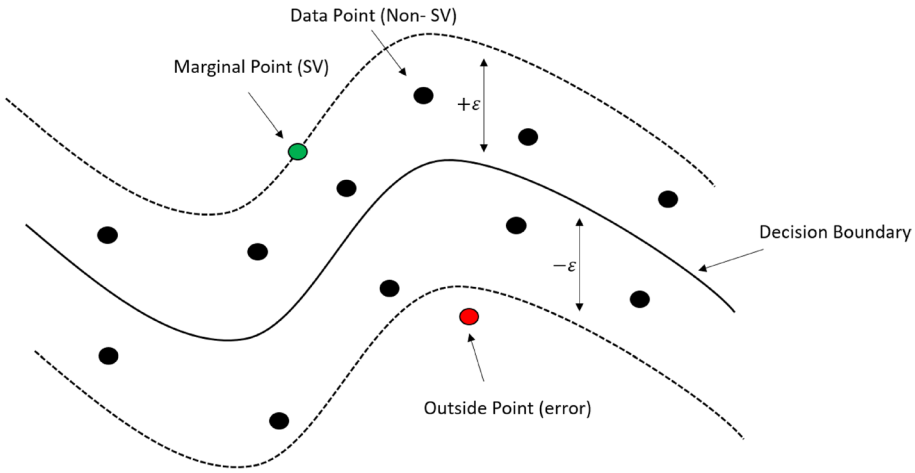

Fig. 8 Schematic diagram of SVR algorithm

We can see in Fig. 9, the distance between the brown point and all other points is calculated then we find the nearest neighbours by ranking points by increasing distance. The nearest neighbours (NN) of the brown point are the ones closest in dataspace.

Extreme Gradient Boosting (XGBoost)

The XGBoost algorithm includes multiple weak decision trees to develop a strong ML model [39]. It is an iterative process where each tree learns from the mistakes of the previous trees to create a better performance. Instead of constructing a series of independent base trees as is the case in Random Forest, XGBoost algorithm builds a scalable end-to-end tree-boosting system as illustrated in Fig. 10. XGBoost helps solving the issue of overfitting in random trees by applying regularization techniques and including a gradient boosting framework which helps in improving the generalization and reducing overfitting [39]. We used the XGBoost library from Python to implement our model.

Numerical study results

In this section, some of the numerical simulation results are presented to help understanding how the features correlate and how bridges' load ratings are affected by truck platooning. The results obtained are for a whole bridge section. However, to obtain the results for individual girders, the output results should be multiplied by the AASHTO live load distribution factors or using the Lever Rule. In addition, Table 3, can be used to account for multiple lane loaded, using multiple presence factor (MPF), according to AASHTO LRFD.

By analyzing these results, we improve understanding of how the presence of truck platooning impacts bridge load ratings, making a vital contribution to existing knowledge in this subject. Furthermore, these findings highlight the value of using ML techniques to aid in the identification and selection of optimal platooning configurations for existing bridges. The efficiency and accuracy of bridge design and maintenance decision-making processes can be improved by employing such algorithms, eventually ensuring the safety and long-term reliability of these key infrastructures.

Truck type

The load effect (bending moment and shear force) of the HS20 design truck model was compared to the load effect of the other five-axle tractor semitrailer trucks that were selected. Figure 11 shows the ratio of the maximum bending moment to the moment generated by the HS20 model for single truck, two-truck platoon, and multi-truck platoon configurations. Similarly, Fig. 12 represents the ratio of the maximum shear force to shear force generated by the HS20 model.

The majority of ratios were found to be less than one, indicating lower load effects as compared to the HS20 design truck. However, two exceptions were identified in the configurations of KYTC and MODOT short trucks, both of which had ratios greater than one. Nonetheless, these increases did not exceed 10% higher than the configurations obtained using the HS20 design truck.

Additionally, it was observed that the ratios decreased as the number of trucks within the platoon increased. With the exception of the two short trucks, this implies that forming a platoon using HS20 design truck model can result in higher bending moments and shear forces compared to five-axle tractor semitrailer trucks.

Number of trucks and headway spacing

Several studies, [20, 22, 23, 25] have highlighted the significance of the number of trucks and headway

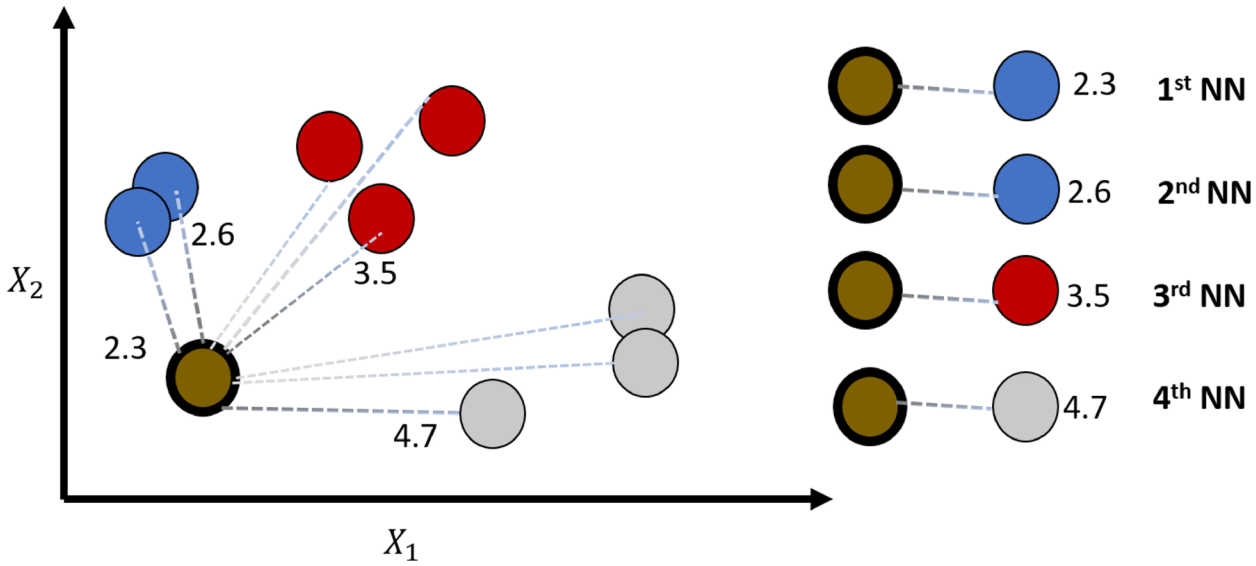

Fig. 9 Schematic diagram of KNN algorithm

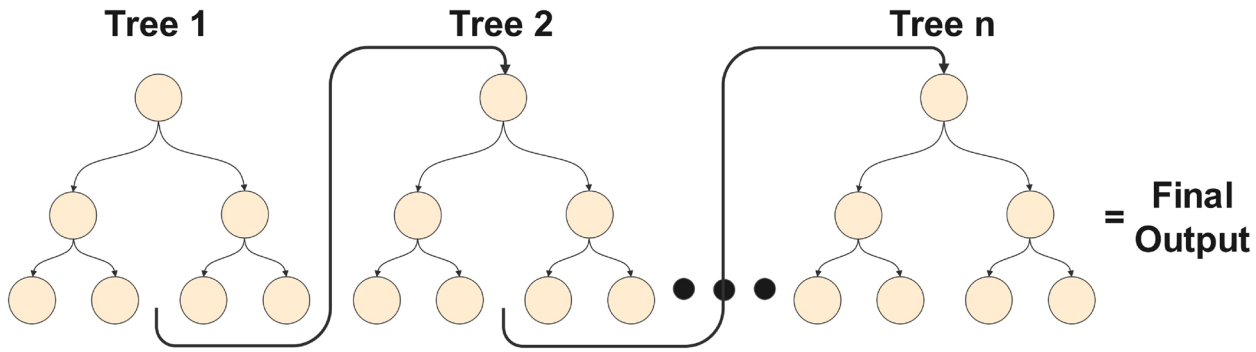

Fig. 10 Schematic diagram of XGBoost algorithm

Table 3 Multiple Presence Factors (MPF) (AASHTO LRFD)

Number of design lanes	Multiple presence factor
1	1.20
2	1.00
3	0.85
More than 3	0.65

spacing as crucial parameters. We investigated the effect of the number of trucks up to 10 trucks and the headway spacing ranging from 8 to 30 ft on bending moments and shear forces of bridges. Figures 13 and 14 show maximum bending moment and shear force results for single, two, and four trucks compared to the HL93 design live load at different headway spacing. Four truck models are shown: the HS20 design truck, the FHWA Class 9, the AASHTO type 3S2, and the MODOT short truck.

When platoons of two, three, or four trucks were considered, our findings revealed significant change in bending moments and shear forces. Platoons formed using two, three, or four FHWA or AASHTO truck models produced bending moments and shear forces within the range of the HL-93 design live load, Figs. 13b, c, 14b, and c. On the other hand, certain four-truck configurations using the HS20 design truck or the MODOT short truck exceeded the design load range obtained by the HL-93, Figs. 13a, d, 14a, and d.

Based on these findings, we recommend adopting the HS20 design truck into bridge designs when considering the platoon effect. The HS20 design truck produced higher load effect compared to the other

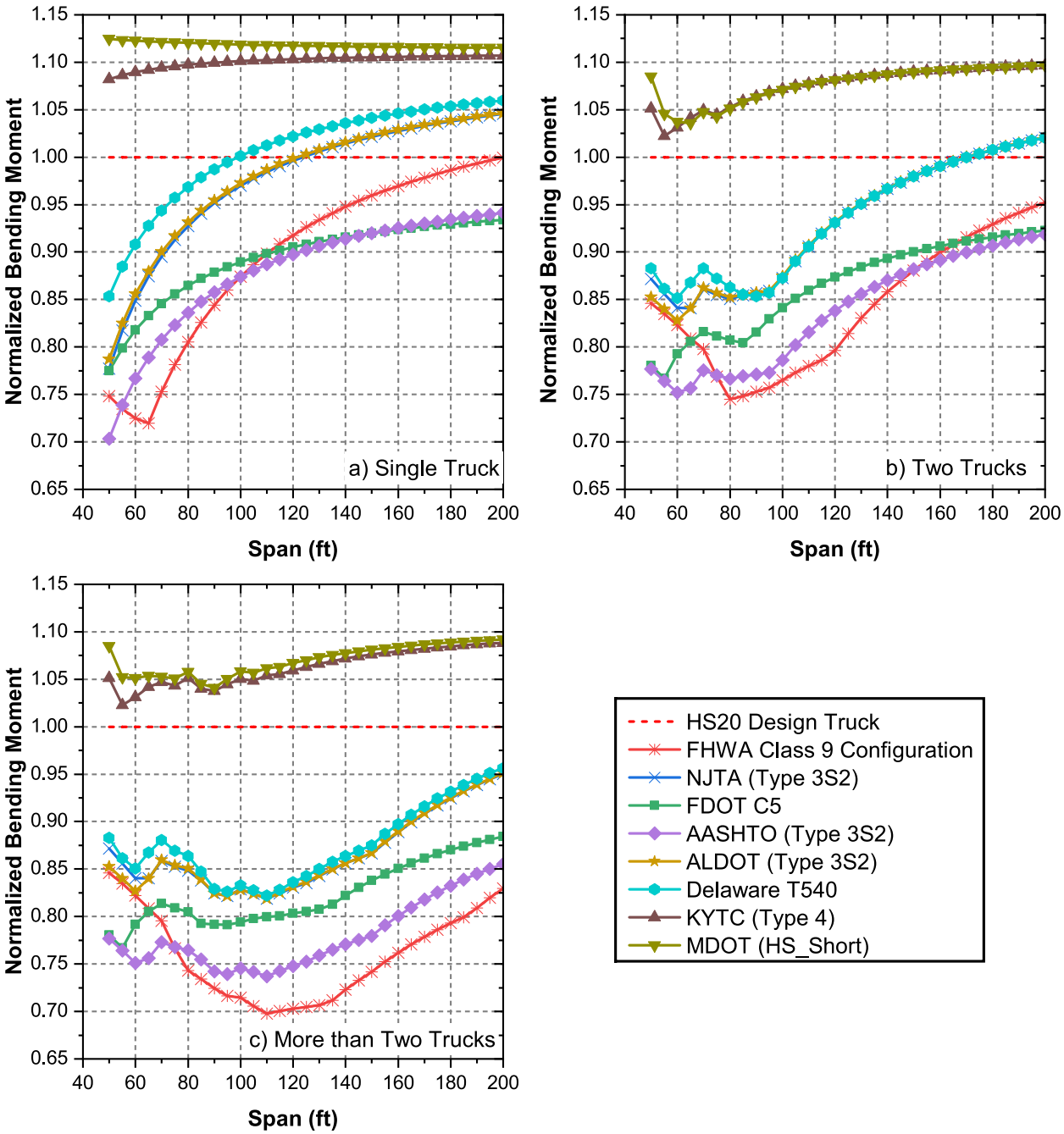

Fig. 11 Normalized bending moments of different truck types compared to the hs20 design truck

models included in our study. Furthermore, our findings highlight the critical need for a simple and effective approach to identify appropriate platoon configurations for current bridges. To address this demand, we suggest the implementation of ML algorithms, which can speed up the identification of critical decision-making parameters.

Bridge continuity

While positive bending moments and end shear forces control simple span bridges, negative bending moments may govern continuous span bridges. As a result, two-, three-, and four-span continuous bridges were evaluated for bending moments and shear forces under various truck platooning configurations. However, when

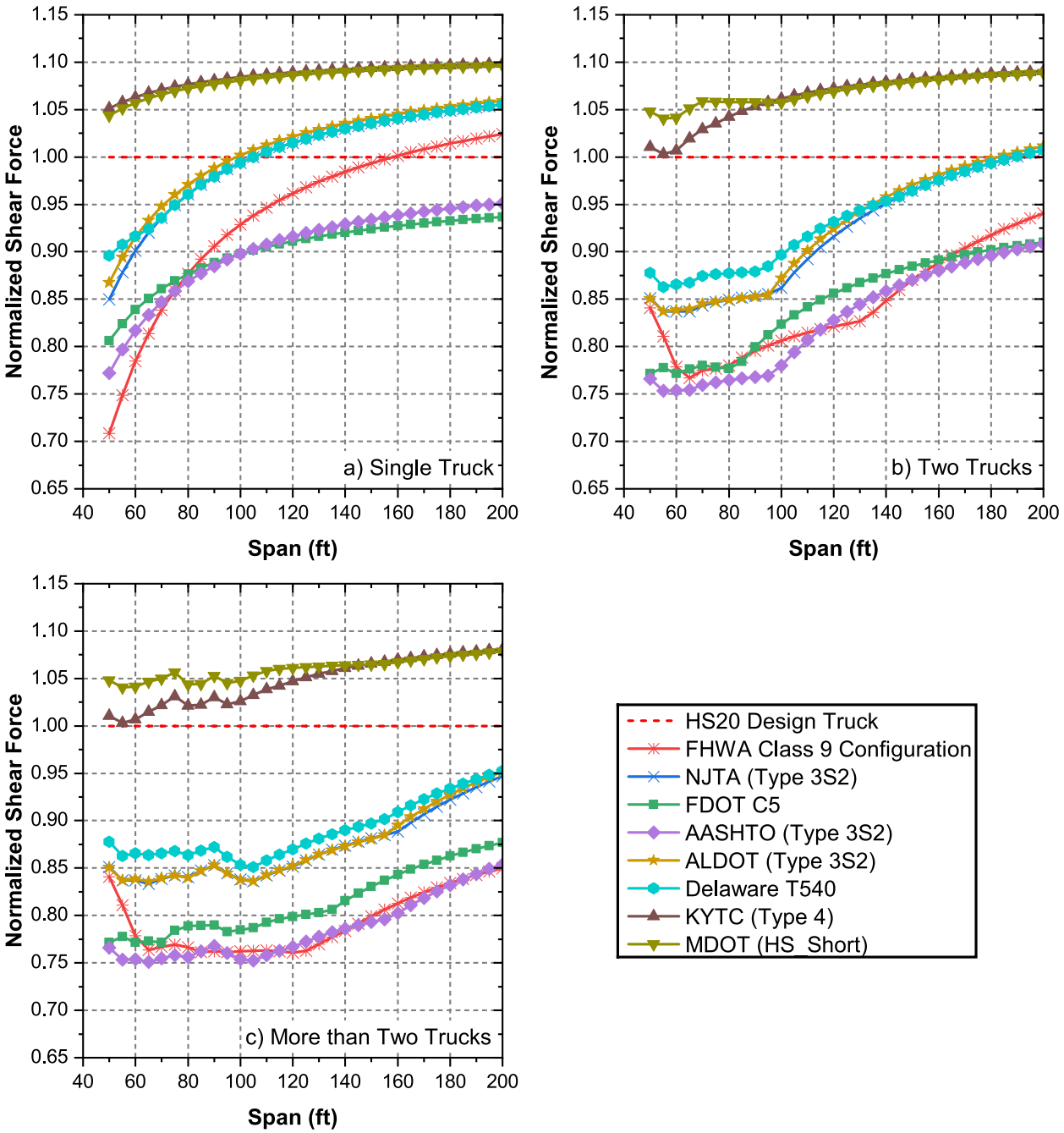

Fig. 12 Normalized Shear Forces of Different Truck Types Compared to the HS20 Design Truck

compared to simple span bridges, continuous span bridges have shown a decrease in positive moments as a result of the development of negative moments. The percentages of positive bending moment reduction due to bridge continuity are primarily affected by the number of spans, span length, and number of trucks.

In our previous study [20, 27], contour plots were developed to calculate the percentage reduction in positive bending moments due to bridge continuity using span length, number of spans, number of trucks, and headway spacing. It was found that the greater the number of spans, the greater the reduction in bending moment. However, all reduction levels were determined to be between 15 and 25%. In this study, ML algorithms were employed to predict the bending moments and shear forces for simple and continuous span bridges.

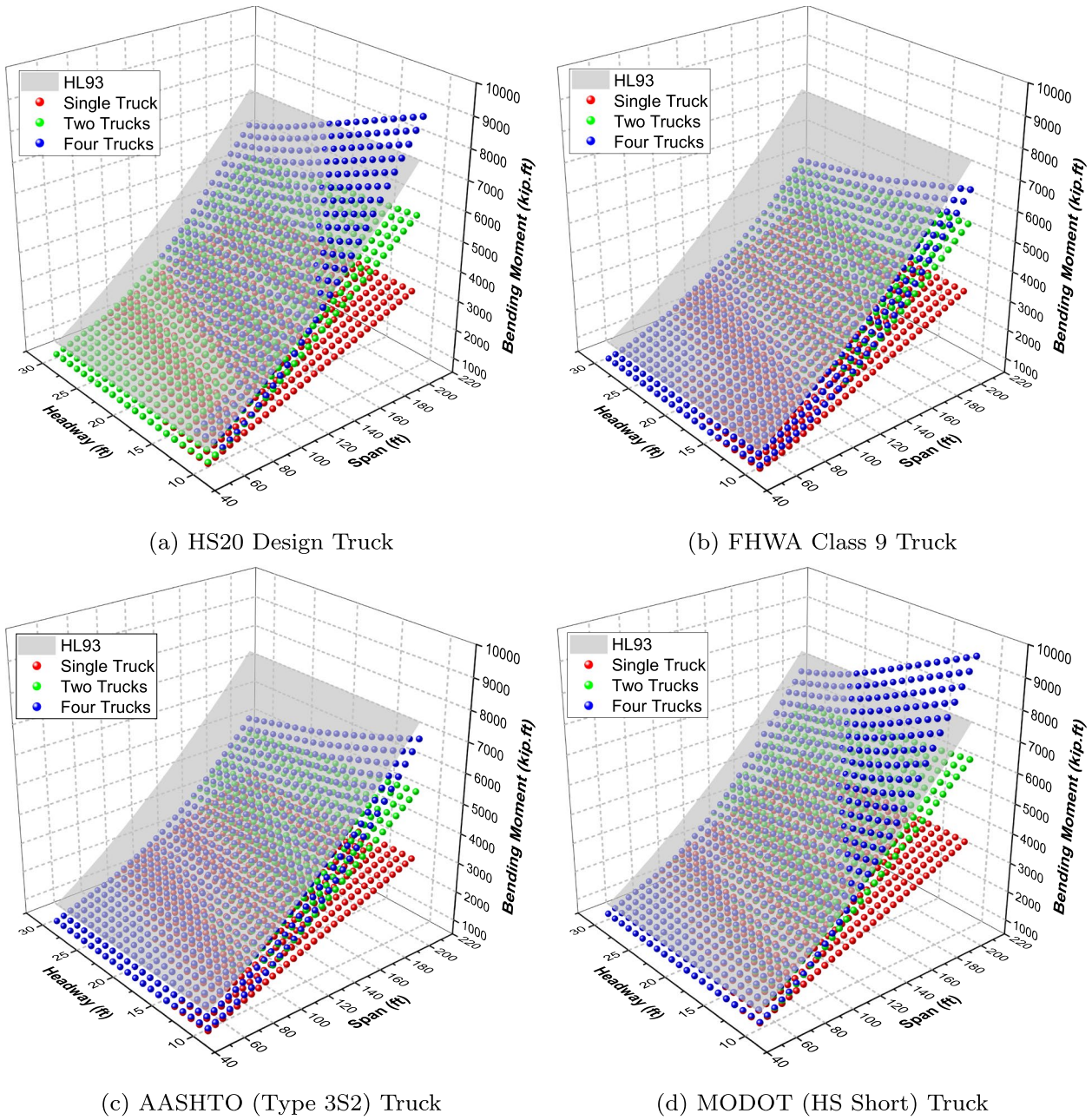

(a) HS20 Design Truck

(b) FHWA Class 9 Truck

(c) AASHTO (Type 3S2) Truck

(d) MODOT (HS Short) Truck

Fig. 13 Maximum bending moment results for single, two, and four trucks compared to the HL93 design live load at different headways

Machine Learning (ML) results

This section evaluates the proposed ML models for regression for the three outputs in terms of the accuracy of the predictions. We start with comparison of the models then we present the accuracy of predictions with the proposed algorithm, Random Forest. Finally, we evaluate the accuracy along different directions with respect to features of truck types, headway, and span lengths.

Comparison of ML models

The first step in our experiments is to analyze the performance of each ML model and choose the best performing model for load rating analysis. To this end, Fig. 15 shows a comparison of the MAE between the actual and predicted outputs of positive, negative bending moments and shear forces using different models. In terms of positive bending moments, the comparison shown in Fig. 15(a) reveals that the Random Forest prediction yields the lowest MAE

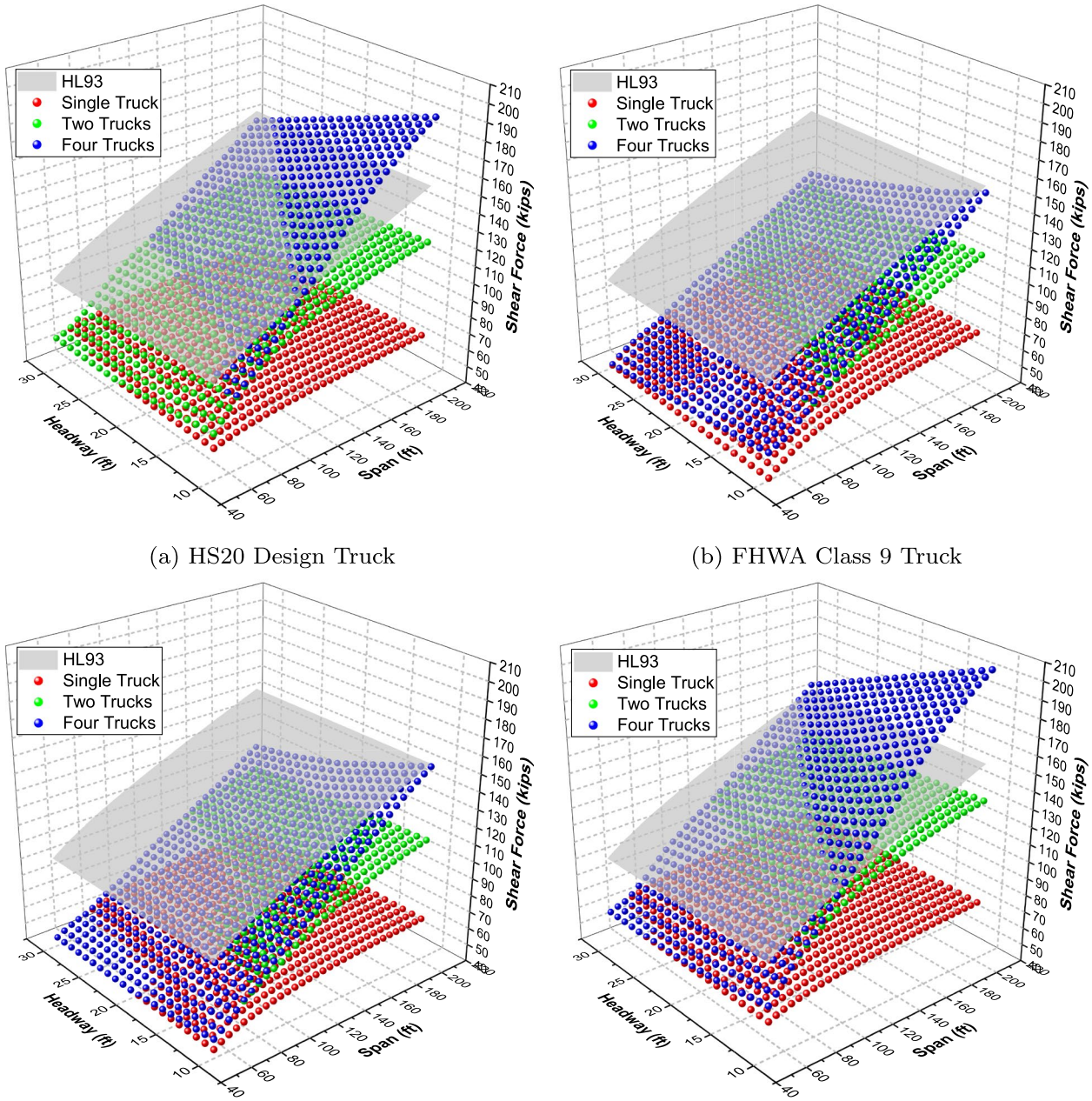

(a) HS20 Design Truck

(b) FHWA Class 9 Truck

(c) AASHTO (Type 3S2) Truck

(d) MODOT (HS Short) Truck

Fig. 14 Maximum shear force results for single, two, and four trucks compared to the HL93 design live load at different headways

as low as 17.63 kip.ft while the SVR prediction gives the highest MAE of 578.64 kip.ft. In terms of negative bending moments, Fig. 15(b), Random Forest maintains its advantage, achieving MAE of 18.69 kip.ft while SVR scores MAE of 426.21 kip.ft. Furthermore, the results of the shear force, Fig. 15(c), show that the MAE of Random Forest is 0.36 kips which gives the lowest MAE among all selected models. This shows that Random Forest has the lowest MAE error among all models.

We computed the RMSE of the predictions using the models as seen in Fig. 16. The predictive performance of the XGBoost and Random Tree models, which are both based on regression trees and gradient boosting, outperforms that of the MLP, SVR, and KNN models; however, Random Forest still gives the lowest RMSE of 22.76 kip.ft, 25.15 kip.ft, and 0.49 kips for positive moment, negative moment, and shear force outputs, respectively.

The correlation coefficients of the prediction were calculated using the models and we found that they all are characterized by quite similar performance of r close to 0.99. The hyperparameters for each model were fine tuned carefully based on a design space exploration. We reported the values that gave the best performance for each model. For example, for the SVR model, we explored four different kernels: RBF, Linear, Poly, and Sigmoid kernel. As can be seen in Tables 4, 5 and 6, we compared the different kernels for positive, negative bending moments and shear forces. We chose the kernel to be RBF because it gives at least three times lower MAE when compared to the Sigmoid kernel. In addition, RBF shows better performance than the Poly kernel and very comparable performance to the linear kernel. RBF is useful in fitting non-linear regression models as explained in "Support Vector Regression (SVR)" section. Therefore, we decided to use RBF because it suits our dataset and has high performance when compared to other kernels.

Comparing the performance of the various ML models discussed in "Machine learning models" section, we determined that Random Forest algorithm exhibits superior results, followed by XGBoost and Random Tree. The MLP and KNN algorithms demonstrated acceptable performance, while SVR had the poorest performance among all models. We also conducted an in-depth analysis of the lowest performance model, SVR, with varying train set proportions compared to Random Forest, the best-performing model, in Tables 7, 8 and 9. We used our study performance measures to illustrate the gap for positive, negative bending moments and shear forces. It was observed that, despite efforts to increase the train set from 60% to 70%, 80%, 90%, and 100% of the dataset, SVR exhibited saturation in performance with a significant gap from the optimal accuracy achieved by Random Forest as seen on the right-most column of the tables in black. Notably, SVR's inability to reach similar accuracies emphasizes the distinct nature of each model and its limitations. Moreover, our decision to employ a 60% train set was based on achieving optimal performance without risking overfitting. The primary goal is to identify a robust model for similar applications, prioritizing high accuracy. Consequently, we chose Random Forest as the primary proposed model. A more comprehensive analysis on the predictions of Random Forest is introduced in the following section.

Accuracy of predictions with random forest

We start the experimental validation of Random Forest algorithm with an analysis of prediction accuracy. To

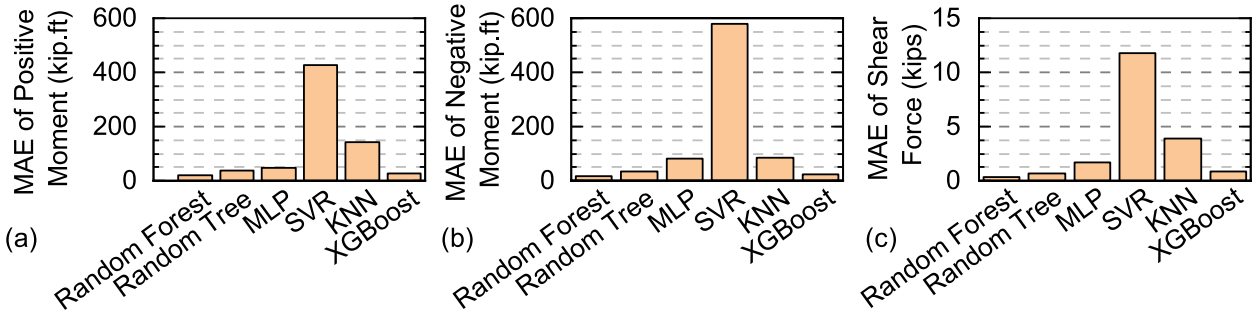

Fig. 15 Comparison of MAE for positive, negative moment and shear force

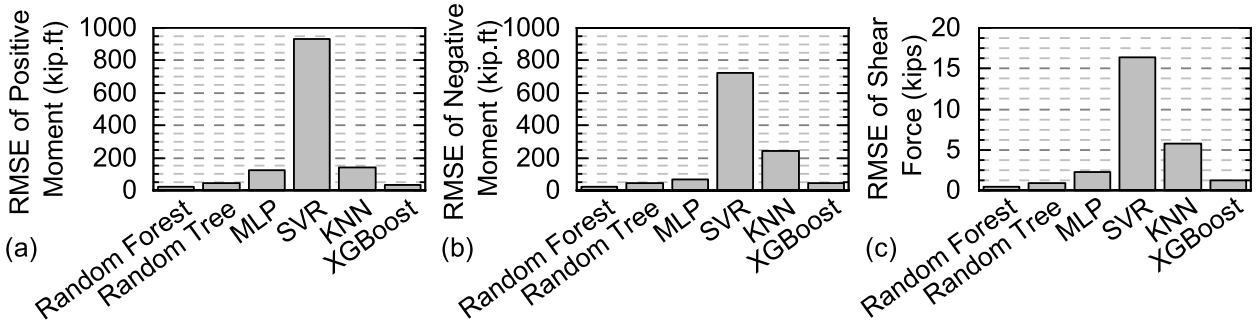

Fig. 16 Comparison of RMSE for positive, negative moment and shear force

Table 4 Comparison between SVR with different kernels for positive bending moments

Kernel	RBF	Linear	Poly	Sigmoid
MAE	426.21	440.03	502.83	2262.8
RMSE	722.15	652.7	739.34	2917.06
r	0.943	0.9	0.93	-0.39

Table 5 Comparison between SVR with different kernels for negative bending moments

Kernel	RBF	Linear	Poly	Sigmoid
MAE	578.64	560.07	661.73	1689.26
RMSE	932.3	820.14	979.11	2261.55
r	0.875	0.9	0.85	-0.13

Table 6 Comparison between SVR with different kernels for shear forces

Kernel	RBF	Linear	Poly	Sigmoid
MAE	11.76	10.02	16.22	1056.17
RMSE	16.42	15.17	20.57	1254.85
r	0.927	0.93	0.88	-0.45

this end, Fig. 17 shows a scatter map of actual data and respective predictions for each point in the dataset. The actual data is shown in red triangle while the prediction is shown in blue circle. It can be seen that the generated output by Random Forest closely matches the actual output. This shows that Random Forest is able to accurately predict the output for the positive moment, negative moment and, shear force respectively. Next, a histogram was constructed to visualize the prediction error. Specifically, the percentage error was computed by the following equation:

$$\text{Percentage Error} = \left| \frac{\text{Predicted Value} - \text{True Value}}{\text{True Value}} \right| \times 100 \quad (8)$$

Figure 18 shows the histogram of the prediction error for all three outputs. We can see that we get a higher error when the output has low magnitude. However, an average prediction error of less than 10% was achieved.

To explore the impact of the features on the prediction output, further examinations were undertaken. Figure 19 shows the scatter matrix of the features, the actual prediction, and the Random Forest prediction for the positive bending moment outputs. The scatter matrix consists of a grid of scatter plots, where each variable is plotted against every other variable [50]. We can see that span length is the feature that impacts the output the most. Results for shear force and negative bending moments have shown the same trend.

Accuracy analysis with truck types, headway, and span lengths

Next, we perform more analysis on number of trucks, headway, span length and bridge type with respect to MAE for all three outputs. The wide range of results caused by different bridge lengths and truck configurations has a significant impact on the model's accuracy. Positive bending moment values in our numerical analysis ranged from 120 kip.ft to 12,580 kip.ft, while negative

Table 7 Comparison between SVR with varying train set proportions and Ranndom Forest for positive bending moments

	SVR					
Percentage of data for train	**60%**	**70%**	**80%**	**90%**	**100%**	**Random Forest**
MAE	426.21	419.8	414.06	409.08	404.86	18.69
RMSE	722.15	711.4	700.94	692.75	686.39	25.15
r	0.943	0.94	0.94	0.94	0.94	0.999

Table 8 Comparison between SVR with varying train set proportions and Ranndom Forest for negative bending moments

	SVR					
Percentage of data for train	**60%**	**70%**	**80%**	**90%**	**100%**	**Random forest**
MAE	578.64	571.3	565.5	560.43	555.8	17.63
RMSE	932.3	921.2	912.5	905.2	898.81	22.76
r	0.875	0.87	0.87	0.87	0.88	0.999

Table 9 Comparison between SVR with varying train set proportions and Ranndom Forest for shear forces

	SVR					
Percentage of data for train	**60%**	**70%**	**80%**	**90%**	**100%**	**Random Forest**
MAE	11.76	11.6	11.46	11.33	11.21	0.36
RMSE	16.42	16.25	16.11	15.98	15.85	0.49
r	0.927	0.92	0.93	0.93	0.93	0.999

bending moments ranged from 110 kip.ft to 9,510 kip.ft. Additionally, the shear forces ranged from 40 kips to 260 kips. As a result, shear forces have shown lower MAE than bending moment results, Figs. 20, 21, and 22. This demonstrates the model's capacity to effectively predict shear forces despite the span lengths and platoon configurations.

Figure 20 shows a 3D plot of number of trucks as X-axis, headway in ft as Y-axis and MAE of the prediction as Z-axis. The increase in the number of trucks coupled with the presence of widely spaced truck platoons creates scenarios in which the entire fleet cannot fit on the bridge, leading to elevated MAE in ML predictions. Furthermore, our analysis was constrained by the absence of instances with headways shorter than 8 ft in the dataset, because those cases are not reliable in real-world scenarios. This lack of data resulted in an increased MAE at headways shorter than 10 ft.

Similarly Fig. 21 visualizes the number of spans on X-axis, the span length on Y-axis and MAE on the Z-axis. The model showed a better predictive performance for simple span bridges, with lower MAE in comparison to continuous bridges. The complexity of continuous bridge analysis, which may accommodate numerous trucks at the same time, resulted in higher MAE. However, the increase in MAE did not exceed 40 kip.ft in all bending moment predictions. Furthermore, instances with short spans, notably those less than 50 ft, had larger errors due to the difficulty of completely accommodating trucks and the requirement for extensive axle analysis in the numerical study; resulting in higher prediction errors.

Finally, we see the correlation between the number of trucks and the span length with respect to the MAE of the prediction in Fig. 22. Notably, the highest MAE is observed when only one truck is present, as a single truck constitutes a relatively small portion of the dataset, due to the absence of some platoon features, such as the number of trucks and headway spacings, which are not applicable when dealing with a single truck.

Potential implementation

Five bridge examples including the case study used in [20] were selected for the purpose of implementation. The bridge in [20] is a 70-ft simple span bridge supported by four W33x130 steel girders, spaced at 7.5 ft. The overall width of the bridge is 25 ft, with 22 ft allocated for the roadway. The bridge has a concrete deck that is 8 in. thick. The interior girder of the bridge was analyzed for moment and shear, resulting in a LRFR rating factors of 1.20 for moment and 2.79 for shear. To allow comparative analysis, additional four bridge cases with span lengths of 100, 120, 150, and 180 ft were included. The parameters

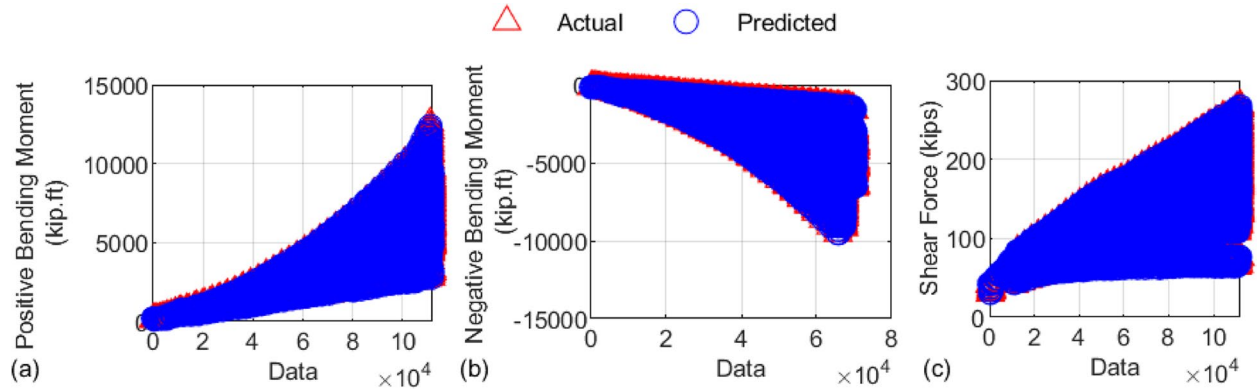

Fig. 17 Actual Vs. Random Forest prediction

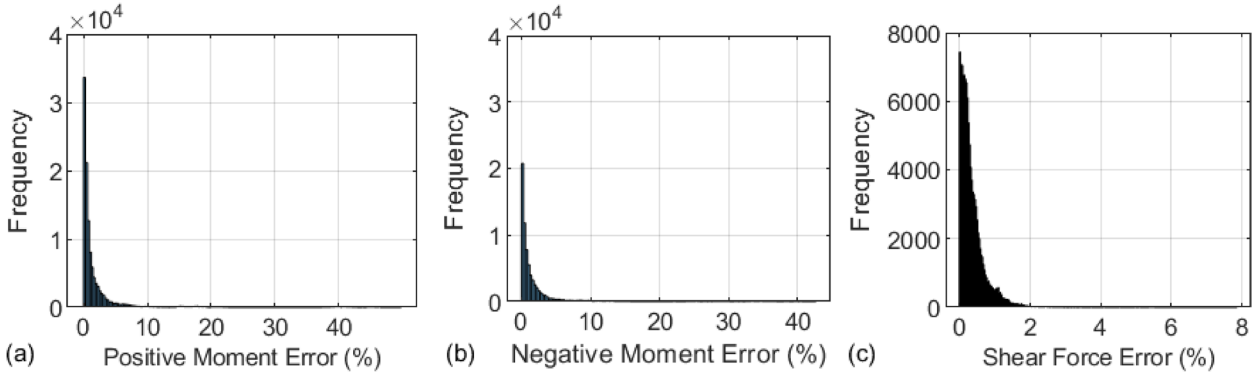

Fig. 18 Percentage Error for **a** positive moment, **b** negative moment, and **c** shear force outputs

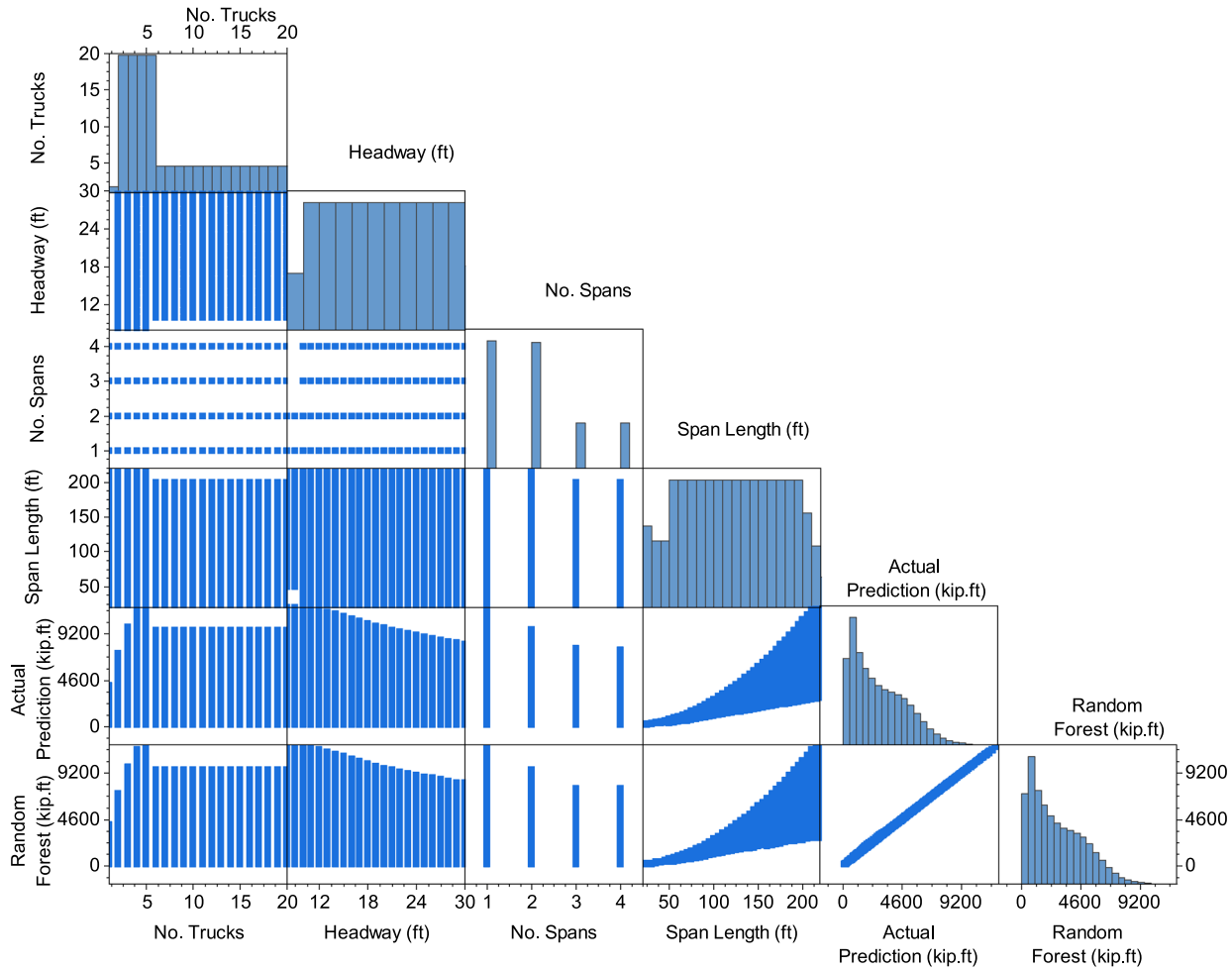

Fig. 19 Scatter matrix of the features, actual prediction and Random Forest prediction for positive bending moments output

for these bridges (capacity, dead loads, and live loads) were selected to produce the same rating factors as the original 70-ft bridge.

ML models were used to find the percentage change in rating factors. Across the five bridge examples, 6,240 predictions were made for bending moments and shear

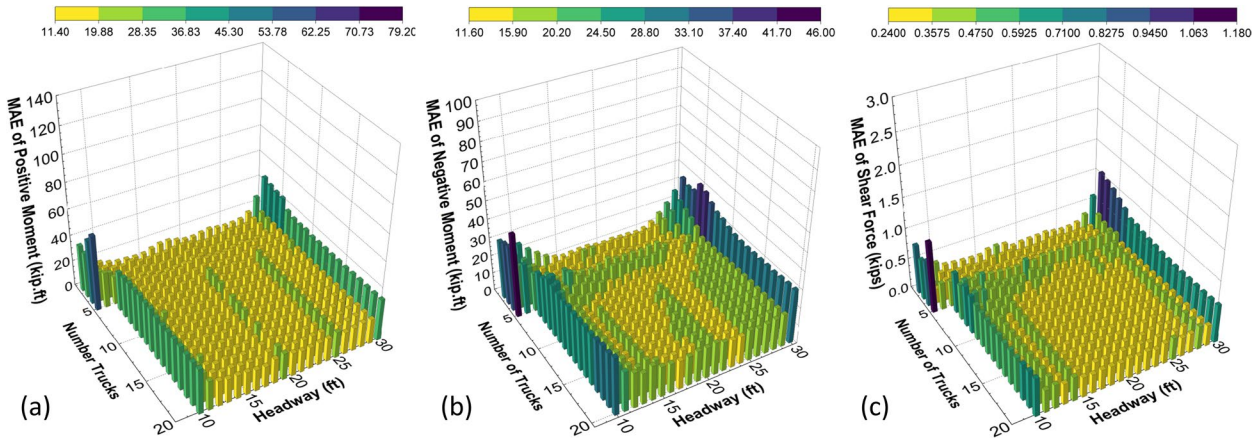

Fig. 20 Mean Absolute Error (MAE) of outputs for number of trucks, and headway

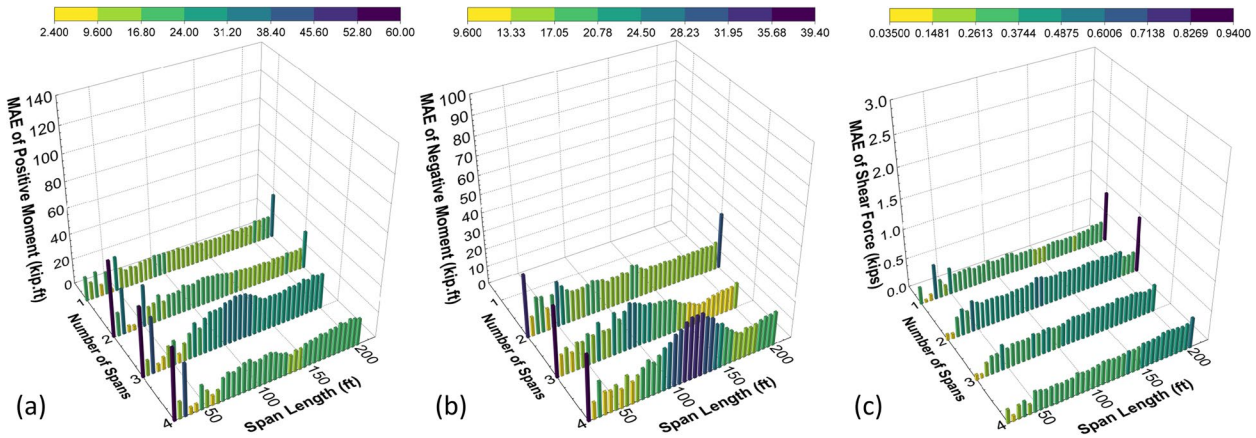

Fig. 21 Mean Absolute Error (MAE) of outputs for number of spans, and span length

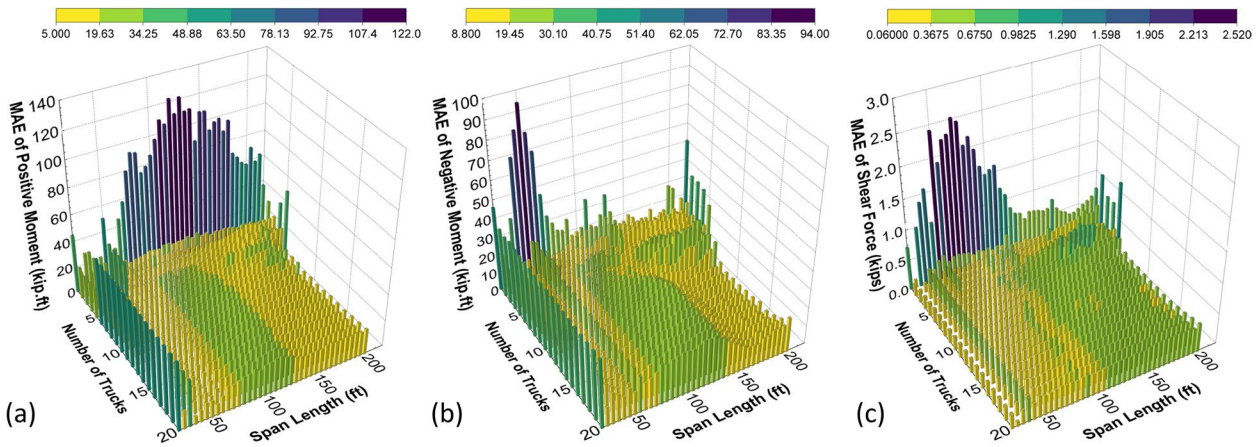

Fig. 22 Mean Absolute Error (MAE) of outputs for number of trucks, and span length

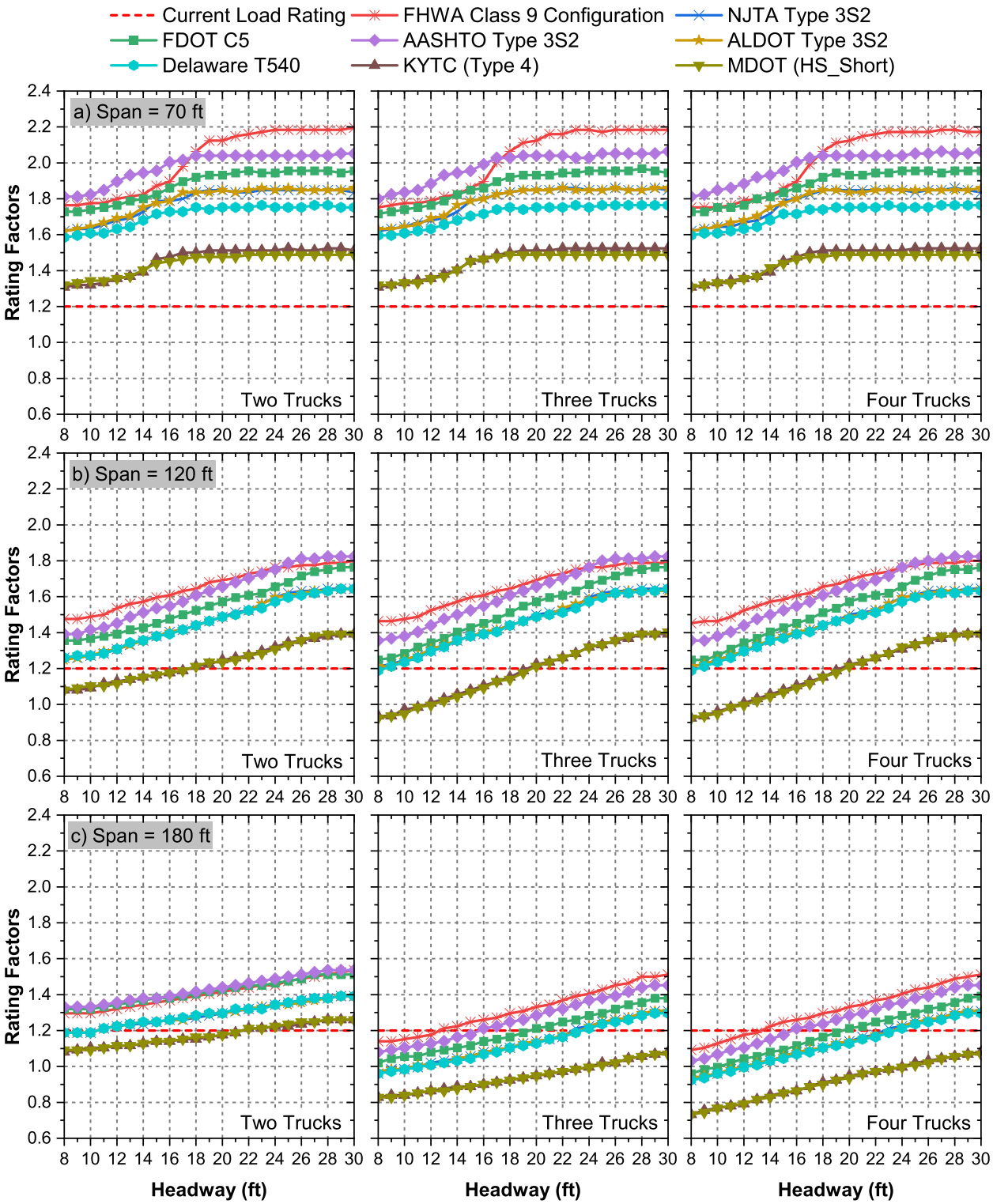

Fig. 23 LRFR rating factors for bending moment predicted using random forest at different truck platooning configurations

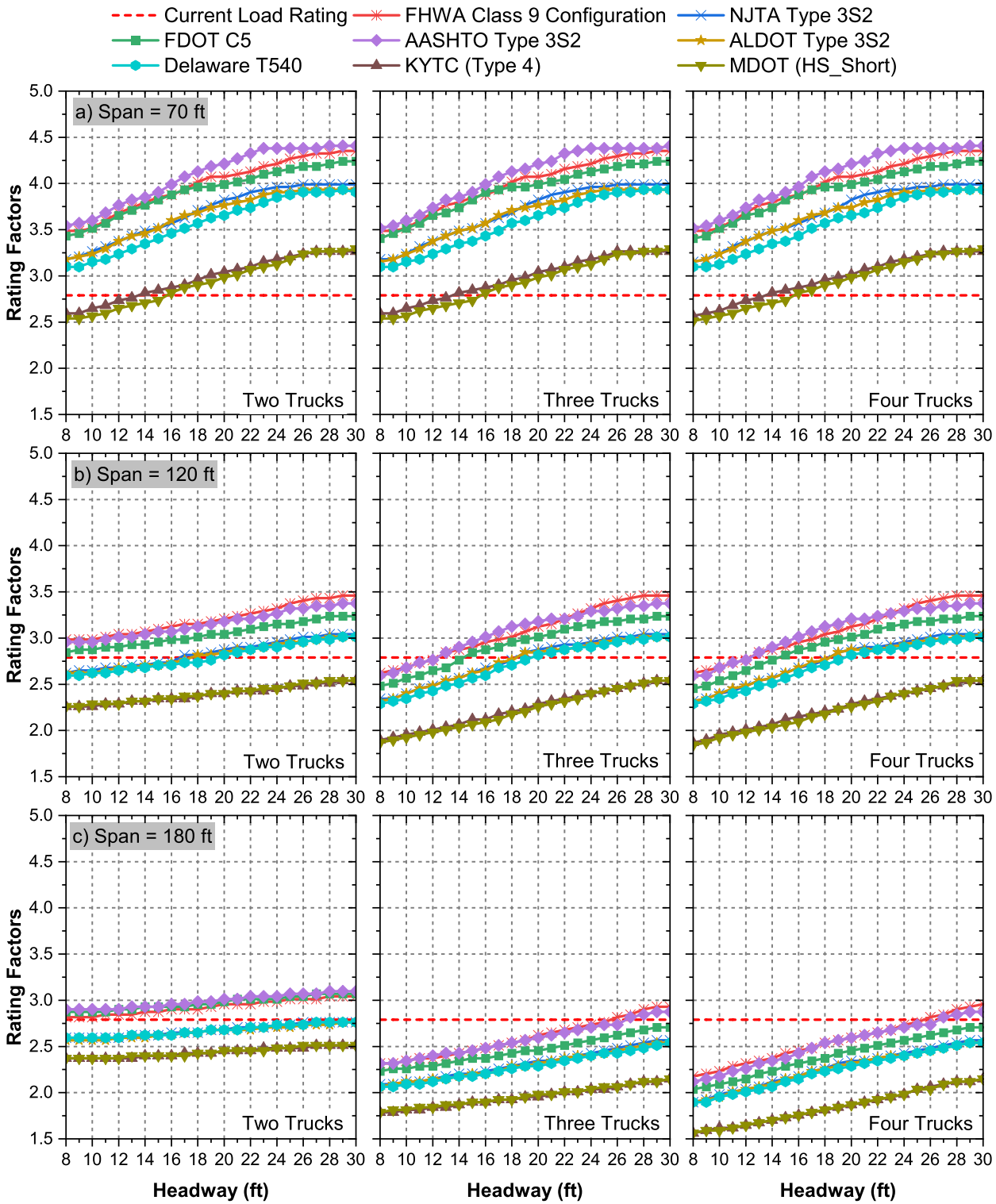

Fig. 24 LRFR rating factors for shear force predicted using random forest at different truck platooning configurations

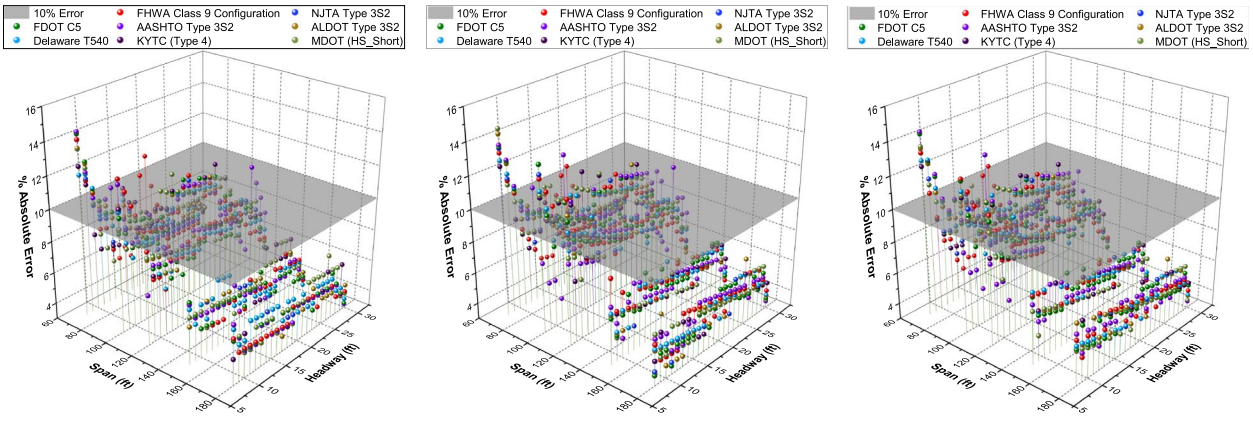

(a) Two Trucks (b) Three Trucks (c) Four Trucks

Fig. 25 Absolute Error results for bending moments' LRFR rating factors at different truck platooning configurations

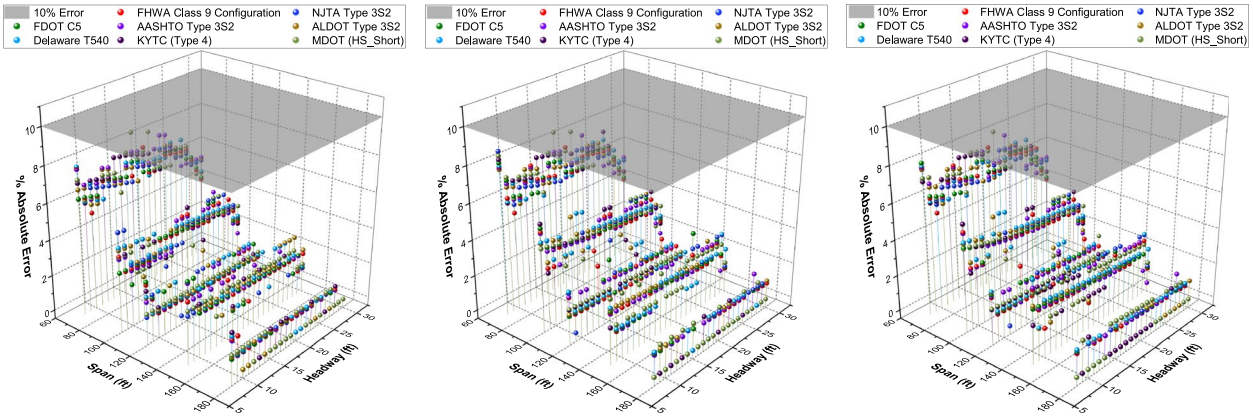

(a) Two Trucks (b) Three Trucks (c) Four Trucks

Fig. 26 Absolute Error results for shear forces' LRFR rating factors at different truck platooning configurations

forces. To obtain the absolute rating factors, we calculated element capacity, and dead loads, based on the given bridge details. Figures 23 and 24 show rating factors for bridges with span lengths of 70, 120, and 180 ft at different truck platooning configurations. Particularly, for the 70-ft bridge, platooning configurations involving two, three, or four trucks, with different truck types and headway spacing, did not result in any reduction in the current rating factors. However, as the span length increases, the platooning effect becomes more apparent, resulting in several platooning configurations that exhibit lower rating factors in comparison to the current rating factor, as can be seen in the 180-ft bridge case. These findings emphasize the significance of utilizing the developed ML approach to identify optimal platooning configurations for bridge structures within the scope of the study.

The validity of ML predictions was established through a rigorous comparison with the results derived numerically using SAP 2000 and Eqs. 1 and 3. The absolute error was calculated using Eq. 9 to measure the difference between the rating factors derived from the random forest predictions and those obtained by implementing the AASHTO LRFR. Figures 25 and 26 show the corresponding absolute error values for the rating factors of the bending moments and shear forces. The results indicate a remarkable level of accuracy, with an absolute error of less than 10% observed for the majority of bending moment rating factors (see Fig. 25) and less than 5% for shear force rating factors (see Fig. 26). These findings confirm the earlier conclusion that higher errors are more likely to occur when the output value (bending moment or shear force) is relatively low. Notably, as the span length

increases, the absolute error decreases, showing a rise in prediction accuracy.

$$\text{Absolute Error} = \left| \frac{\text{Predicted Value} - \text{AASHTO LRFR Value}}{\text{AASHTO LRFR Value}} \right| \times 100 \quad (9)$$

Conclusions

This research work includes a comprehensive parametric study using SAP 2000 to assess the impact of different truck platooning configurations on the load rating of existing bridges. The study involved 295,200 computer simulations to address various parameters such as the number of bridge spans, span lengths, truck type, number of truck platoons, and spacing between trucks (headway). The obtained results served as the dataset for training various ML models, including Random Tree, Random Forest, Multi-Layer Perceptron (MLP), Support Vector Regression (SVR), K-Nearest Neighbor (KNN), and Extreme Gradient Boosting (XGBoost).

The primary findings were:

- The type of trucks significantly affect the bending moments and shear forces. The majority of ratios were found to be less than one, indicating lower load effects as compared to the HS20 design truck. However, two exceptions were identified in the configurations of KYTC and MDOT short trucks, both of which had ratios greater than one. Nonetheless, these increases did not exceed 10% higher than the configurations obtained using the HS20 design truck.
- Forming a platoon using HS20 design truck model can result in higher bending moments and shear forces compared to five-axle tractor semi-trailer trucks. Consequently, we recommend adopting the HS20 design truck into bridge designs when considering the platoon effect, as it produces higher load effects compared to the majority of the models studied.
- The findings highlight the crucial need for a simple and effective method for determining optimal platoon configurations for existing bridges. To address this demand, we suggest the implementation of ML algorithms, which can speed up the identification of critical decision-making parameters.
- Random Forest was selected as the primary proposed ML model because it showed the best performance with the lowest prediction errors and used its prediction to carry out more analysis with respect to the input features.
- The results of the five bridge case studies had an absolute error of less than 10% for the majority of bending moment LRFR rating factors and less than 5% for shear force LRFR rating factors.

Authors' contributions
M.E. and D.H. wrote the main manuscript text and M.E, and D.H prepared all figures. A.I, A.A, and G.B. have contributed to the originality of the research and the techniques and simulations that have been conducted. All authors reviewed the manuscript.

Funding
This project has been funded by the Pacific Northwest Transportation Consortium, University Transportation Center for Federal Region 10, University of Washington, grant 69A355174110.

Availability of data and materials
No datasets were generated or analysed during the current study.

Declarations

Ethics approval and consent to participate
Not applicable.

Competing interests
The authors declare no competing interests.

Author details
[1]Department of Civil and Environmental Engineering, University of Idaho, Moscow, ID 83844-1022, USA. [2]School of Electrical Engineering and Computer Science, Washington State University, Pullman, WA 99164, USA. [3]Department of Civil and Environmental Engineering, University of Missouri, Columbia, USA.

Received: 12 December 2023 Revised: 22 February 2024 Accepted: 1 March 2024
Published online: 07 April 2024

References

1. Gungor OE, She R, Al-Qadi IL, Ouyang Y (2020) One for all: decentralized optimization of lateral position of autonomous trucks in a platoon to improve roadway infrastructure sustainability. Transp Res C Emerg Technol 120:102783
2. Agency IE (2022) IEA energy and carbon tracker 2022. IEA
3. Gungor OE, Al-Qadi IL, Gamez A, Hernandez JA (2016) In-situ validation of three-dimensional pavement finite element models. In: The roles of accelerated pavement testing in pavement sustainability: engineering, environment, and economics, Springer, pp 145–159
4. Suzuki Y (2011) A new truck-routing approach for reducing fuel consumption and pollutants emission. Transp Res D Transp Environ 16(1):73–77
5. Gungor OE, She R, Al-Qadi IL, Ouyang Y, et al (2018) Optimization of lateral position of autonomous trucks. Tech. Rep., University of Michigan. Center for Connected and Automated Transportation
6. Browand F, McArthur J, Radovich C (2004) Fuel saving achieved in the field test of two tandem trucks. California Path Programinstitute of Transportation Studies University of California, Berkeley, p 1–30
7. Bergenhem C, Shladover S, Coelingh E, Englund C, Tsugawa S (2012) Overview of platooning systems. In: Proceedings of the 19th ITS World Congress, Vienna, p 1–8
8. Bishop R (2017) Connected automated trucking: latest developments and outlook. 5th Annual Florida Automated Vehicles (FAV) Summit, p 14–15
9. Kuhn B, Lukuc M, Poorsartep M, Wagner J, Balke KN, Middleton D, Songchitruksa P, Wood N, Moran M, et al (2017) Commercial truck

platooning demonstration in texas–level 2 automation. Tech. Rep., Texas. Dept. of Transportation. Research and Technology Implementation Office
10. Jacob B, de Chalendar OA (2018) Truck platooning: expected benefits and implementation conditions on highways. In: Heavy Vehicle Transportant Technology (HVTT) International Symposium, p 1–11. https://hvttforum.org/wp-content/uploads/2019/11/Jacob-TRUCK-PLATOONING-EXPECTED-BENEFITS-AND-IMPLEMENTATION-CONDITIONS-ON-HIGHWAYS.pdf
11. Birgisson B, Morgan CA, Yarnold M, Warner J, Glover B, Steadman MP, Srinivasa S, Cai S, Lee D, et al (2020) Evaluate potential impacts, benefits, impediments, and solutions of automated trucks and truck platooning on texas highway infrastructure: Technical Report. Texas. Dept. of Transportation. Research and Technology Implementation Office
12. Saeed TU, Alabi BN, Labi S (2021) Preparing road infrastructure to accommodate connected and automated vehicles: system-level perspective. J Infrastruct Syst 27(1):06020003
13. Calvert S, Schakel WJ, van Arem B (2019) Evaluation and modelling of the traffic flow effects of truck platooning. Transp Res C Emerg Technol 105:1–22
14. Zabat M, Stabile N, Farascaroli S, Browand F (1995) The aerodynamic performance of platoons: a final report. California Path Program Institute of Transportation Studies University of California, Berkeley
15. Gaudet B, Eng P (2014) Technical report review of cooperative truck platooning systems. Technical Report
16. Tsugawa S, Jeschke S, Shladover SE (2016) A review of truck platooning projects for energy savings. IEEE Trans Intell Veh 1(1):68–77
17. Bonnet C, Fritz H (2000) Fuel consumption reduction in a platoon: experimental results with two electronically coupled trucks at close spacing. Tech. Rep, SAE Technical Paper
18. Michaelian M, Browand F (2001) Quantifying platoon fuel savings: 1999 field experiments. SAE Trans 110:1401–1410
19. Sayed SM, Sunna HN, Moore PR (2020) Truck platooning impact on bridge preservation. J Perform Constr Facil 34(3):04020029
20. Elshazli MT, Ibrahim A, Abdel-Rahim A (2023) Truck platooning impact on existing bridges' load ratings. Structures, Elsevier 51:1706–1721
21. DeVault A, Beitelman T (2017) Two-truck platooning: load Effects of Two-Truck Platoons on Interstate and Turnpike Bridges in Florida
22. Kamranian Z (2018) Load evaluation of the hay river bridge under different platoons of connected trucks. Master's thesis, Graduate Studies
23. Yarnold MT, Weidner JS (2019) Truck platoon impacts on steel girder bridges. J Bridg Eng 24(7):06019003
24. Tohme R, Yarnold M (2020) Steel bridge load rating impacts owing to autonomous truck platoons. Transp Res Rec 2674(2):57–67
25. Thulaseedharan NP, Yarnold MT (2020) Prioritization of texas prestressed concrete bridges for future truck platoon loading. Bridg Struct 16(4):155–167
26. Couto Braguim T, Lou P, Nassif H (2021) Truck platooning to minimize load-induced fatigue in steel girder bridges. Transp Res Rec 2675(4):146–154
27. Elshazli M, Ibrahim A, Abdel-Rahim A, Consortium PNT, et al (2022) Impact of autonomous and connected truck platoons in the pacific northwest on transportation infrastructure. Tech. Rep., Pacific Northwest Transportation Consortium (PacTrans)(UTC)
28. Ibrahim A, Abdel Rahim A, Elshazli M (2022) Impact of autonomous and connected truck platoons in the pacific northwest on transportation infrastructure. Tech. Rep, Pacific Northwest Transportation
29. Almustafa MK, Nehdi ML (2022) Machine learning model for predicting structural response of RC columns subjected to blast loading. Int J Impact Eng 162:104145
30. Hussein D, Bhat G (2023) Sensorgan: A novel data recovery approach for wearable human activity recognition. ACM Trans Embed Comput Syst. https://dl.acm.org/doi/abs/10.1145/3609425
31. Lai D, Demartino C, Xiao Y (2023) Interpretable machine-learning models for maximum displacements of RC beams under impact loading predictions. Eng Struct 281(115):723
32. Hussein D, Belkhouja T, Bhat G, Doppa JR (2022) Reliable machine learning for wearable activity monitoring: Novel algorithms and theoretical guarantees. In: Proceedings of the 41st IEEE/ACM International Conference on Computer-Aided Design, pp 1–9. https://dl.acm.org/doi/abs/10.1145/3508352.3549430
33. Bhat G, Hussein D, Yamin N (2023) Robust machine learning for low-power wearable devices: challenges and opportunities. Embedded Machine Learning for Cyber-Physical, IoT, and Edge Computing: Use Cases and Emerging Challenges. Springer, pp 45–71. https://link.springer.com/chapter/10.1007/978-3-031-40677-5_3
34. Ho TK (1998) The random subspace method for constructing decision forests. In: IEEE Transactions on Pattern Analysis and Machine Intelligence, vol. 20, no. 8. IEE, pp. 832–844. https://ieeexplore.ieee.org/abstract/document/709601
35. Breiman L (2001) Random forests. Mach Learn 45:5–32
36. Rumelhart DE, Hinton GE, Williams RJ (1986) Learning representations by back-propagating errors. Nature 323(6088):533–536
37. Drucker H, Burges CJC, Kaufman L, Smola A, Vapnik V (1996) Support Vector Regression Machines. In: Mozer MC, Jordan M, Petsche T (eds) Advances in Neural Information Processing Systems, vol 9. MIT Press. https://proceedings.neurips.cc/paper_files/paper/1996/file/d38901788c533e8286cb6400b40b386d-Paper.pdf
38. Altman NS (1992) An introduction to kernel and nearest-neighbor nonparametric regression. Am Stat 46(3):175–185
39. Chen T, Guestrin C (2016) Xgboost: A scalable tree boosting system. In: Proceedings of the 22nd ACM SIGKDD International Conference on Knowledge Discovery and Data Mining, Association for Computing Machinery, New York, p 785–794. https://doi.org/10.1145/2939672.2939785
40. Nowak AS, Nassif H, DeFrain L (1993) Effect of truck loads on bridges. J Transp Eng 119(6):853–867
41. Ghosn M (2000) Development of truck weight regulations using bridge reliability model. J Bridg Eng 5(4):293–303
42. James R, Noel J, Furr L, Bonilla F (1985) Proposed new truck weight formula. Rep No FHWA/RD-85/088, Federal Highway Administration, Washington
43. Wassef W, et al (2021) Truck platooning impacts on bridges: Phase i–structural safety. Tech. Rep., United States Department of Transportation. Intelligent Transportation Systems Joint Program Office
44. Yang B, Steelman JS, Puckett JA, Linzell DG (2021) Safe platooning headways on girder bridges. Transp Res Rec 03611981211036379. https://doi.org/10.1177/03611981211036379
45. Witten IH, Frank E, Hall MA, Pal CJ (2016) Data Mining, 4th edn. Practical Machine Learning Tools and Techniques, Morgan Kaufmann Publishers Inc
46. Pedregosa F, Varoquaux G, Gramfort A, Michel V, Thirion B, Grisel O, Blondel M, Prettenhofer P, Weiss R, Dubourg V, Vanderplas J, Passos A, Cournapeau D, Brucher M, Perrot M, Duchesnay E (2011) Scikit-learn: machine learning in Python. J Mach Learn Res 12:2825–2830
47. Chen T, Guestrin C (2016) XGBoost: a scalable tree boosting system. In: Proceedings of the 22nd ACM SIGKDD International Conference on Knowledge Discovery and Data Mining, ACM, KDD '16, pp 785–794. https://doi.org/10.1145/2939672.2939785
48. Potdar K, Pardawala TS, Pai CD (2017) A comparative study of categorical variable encoding techniques for neural network classifiers. Int J Comput Appl 175(4):7–9
49. Dar Y, Muthukumar V, Baraniuk RG (2021) A farewell to the bias-variance tradeoff? an overview of the theory of overparameterized machine learning. arXiv preprint arXiv:2109.02355
50. Waskom ML (2021) Seaborn: statistical data visualization. J Open Source Softw 6(60):3021. https://doi.org/10.21105/joss.03021

Publisher's Note